

GW and beyond : application to SiC, Si, C

Citation for published version (APA):

Ummels, R. T. M. (1998). *GW and beyond : application to SiC, Si, C*. [Phd Thesis 1 (Research TU/e / Graduation TU/e), Applied Physics and Science Education]. Technische Universiteit Eindhoven.
<https://doi.org/10.6100/IR515462>

DOI:

[10.6100/IR515462](https://doi.org/10.6100/IR515462)

Document status and date:

Published: 01/01/1998

Document Version:

Publisher's PDF, also known as Version of Record (includes final page, issue and volume numbers)

Please check the document version of this publication:

- A submitted manuscript is the version of the article upon submission and before peer-review. There can be important differences between the submitted version and the official published version of record. People interested in the research are advised to contact the author for the final version of the publication, or visit the DOI to the publisher's website.
- The final author version and the galley proof are versions of the publication after peer review.
- The final published version features the final layout of the paper including the volume, issue and page numbers.

[Link to publication](#)

General rights

Copyright and moral rights for the publications made accessible in the public portal are retained by the authors and/or other copyright owners and it is a condition of accessing publications that users recognise and abide by the legal requirements associated with these rights.

- Users may download and print one copy of any publication from the public portal for the purpose of private study or research.
- You may not further distribute the material or use it for any profit-making activity or commercial gain
- You may freely distribute the URL identifying the publication in the public portal.

If the publication is distributed under the terms of Article 25fa of the Dutch Copyright Act, indicated by the "Taverne" license above, please follow below link for the End User Agreement:

www.tue.nl/taverne

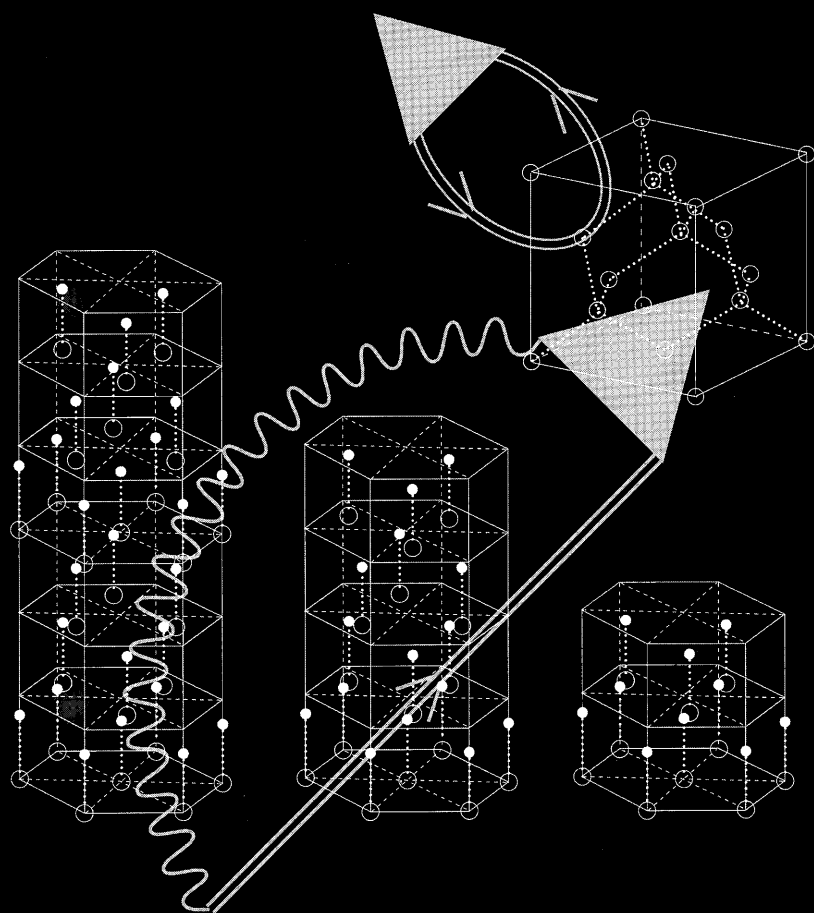
Take down policy

If you believe that this document breaches copyright please contact us at:

openaccess@tue.nl

providing details and we will investigate your claim.

GW and beyond: application to SiC, Si, C



R.T.M. Ummels

***GW* and beyond: application to SiC, Si, C**

PROEFSCHRIFT

ter verkrijging van de graad van doctor aan de
Technische Universiteit Eindhoven, op gezag van de
Rector Magnificus, prof.dr. M. Rem, voor een
commissie aangewezen door het College voor
Promoties in het openbaar te verdedigen op
dinsdag 27 oktober 1998 om 16.00 uur

door

René Theodorus Marie Ummels

geboren te Maastricht

Dit proefschrift is goedgekeurd
door de promotoren:
prof.dr. W. van Haeringen
en
prof.dr. M.A.J. Michels

Copromotor:
dr. P.A. Bobbert

Druk: Universiteitsdrukkerij, Technische Universiteit Eindhoven

CIP-DATA LIBRARY TECHNISCHE UNIVERSITEIT EINDHOVEN

Ummels, René Theodorus Marie

GW and beyond: application to SiC, Si, C / by René Theodorus Marie Ummels. -
Eindhoven: Technische Universiteit Eindhoven, 1998. - Proefschrift. -
ISBN 90-386-0717-2

NUGI 812

Trefw.: quantummechanica / halfgeleiders; bandenstructuur / halfgeleiders; elektronen-
structuur

Subject headings: quantum mechanics / semiconductors; band structure / semiconductors;
electronic structure

René Ummels
Physics Department
Eindhoven University of Technology
P.O. Box 513
5600 MB Eindhoven
The Netherlands

The work described in this thesis was carried out at the Physics Department of the Eindhoven University of Technology. It was supported by the National Computing Facilities Foundation (NCF) for the use of supercomputer facilities, with financial support from the Netherlands Organization for Scientific Research (NWO).

Contents

Samenvatting	3
Summary	5
1 Introduction	9
1.1 The success of the <i>GW</i> theory	10
1.2 Why is the <i>GW</i> theory so successful?	12
2 Theory	15
2.1 Introduction	15
2.2 The Hamiltonian of the many-electron system	16
2.3 Density-functional theory	17
2.4 Quasiparticle theory	18
2.4.1 Green's function theory	19
2.4.2 Hedin's scheme	20
2.4.3 Quasiparticle band structure	22
2.4.4 The <i>GW</i> approach	23
2.4.5 Higher-order corrections	24
3 Ab initio quasiparticle energies in 2H, 4H, and 6H SiC	27
3.1 Introduction	27
3.2 Theory	28
3.3 Results	30
3.4 Conclusion	33
4 First-order corrections to RPA-GW calculations in silicon and diamond.	37
4.1 Introduction	37
4.2 Theory	40
4.3 Results	45
4.3.1 First-order corrections to the RPA polarizability	46
4.3.2 First-order corrections to the <i>GW</i> self-energy	49

Contents

4.4	Checks	51
4.5	Discussion on the self-consistency self-energy diagrams	53
4.6	A remarkable cancellation	54
4.7	Discussion and conclusions	56
A	The expression for a polarizability correction subdiagram	61
	Bibliography	63

Samenvatting

De in de jaren zestig opgestelde zogeheten *GW*-theorie geeft een kwantummechanische beschrijving van geëxciteerde elektron toestanden in een systeem met wisselwerkende elektronen. Sinds het einde van de jaren tachtig is duidelijk geworden dat de *GW*-theorie een verrassend goed raamwerk biedt voor het berekenen van bandstructuren. In het bijzonder blijken de in dit kader berekende elektron energiebanden rondom de bandgap, de energiekloof tussen de elektron energieën van de bezette elektron toestanden in de grondtoestand van het bekeken systeem en de geëxciteerde elektron toestanden, tot uitstekende overeenstemming te leiden met experimentele gegevens voor een grote groep halfgeleiders. Eerdere schema's zoals het Hartree en het Hartree-Fock schema geven deze overeenstemming duidelijk niet. Ook de dichtheidsfunctionaaltheorie, ondanks haar succesvolle beschrijving van de grondtoestandseigenschappen van halfgeleiders, leidt niet tot bevredigende resultaten in het geval van halfgeleiders als het gaat om de bandstructuur rondom de bandgap. In dit proefschrift wordt in de eerste plaats nagegaan of de *GW*-theorie eveneens tot goede resultaten leidt als deze wordt toegepast op drie polytypen van siliciumcarbide, te weten 2H, 4H en 6H siliciumcarbide, halfgeleiders met respectievelijk 4, 8 en 12 atomen in de primitieve eenheidscel. We laten zien dat ook voor deze relatief gecompliceerde halfgeleiders de *GW*-theorie tot uitstekende overeenstemming met het experiment leidt. Hierbij dient te worden opgemerkt dat in het door ons gehanteerde algoritme gebruik is gemaakt van een plasmon-pool model, dat in een analytische benadering voorziet voor de energie-afhankelijkheid van de dynamisch afgeschermd elektron-elektron wisselwerking *W*. Er kan dus worden geconcludeerd dat de *GW*-theorie, in samenhang met dit plasmon-pool model, tot uitstekende overeenstemming leidt met het experiment, zelfs als het om deze gecompliceerde halfgeleiders gaat.

In de tweede plaats richt het proefschrift zich op de vraag waarom de *GW*-theorie klaarblijkelijk zo succesvol is. De leidende gedachte daarbij is dat de essentiële bijdrage tot de elektron energieën in deze theorie wordt verkregen door een storingsreeks in termen van *W* na laagste orde af te kappen. Deze storingsreeks volgt uit een theorie waarin het totale effect van de elektron-elektron wisselwerking op de elektron energieën voorgesteld kan worden als een oneindige som van zogeheten Feynman diagrammen. In de *GW*-theorie worden dus de hogere orde diagrammen verwaarloosd. Het is echter niet *a priori* duidelijk hoe het met de convergentie van de storingsreeks is gesteld. Echter, recente berekeningen voor het geval van het homogene elektron gas door Shirley, alsmede voor het geval van een één-dimensionale modelhalfgeleider leverden een geringe bijdrage op van de eerstvolgende diagrammen in de storingsreeks. Iets nauwkeuriger: voor de één-dimensionale modelhalfgeleider werden de laagste orde diagrammen berekend, die zogenoemde "zelfconsistentie" en "vertex correctie" bijdragen bevatten, en er werd gevonden dat die elkaar in hoge mate com-

penseren. Voor het homogene elektron gas werd door Shirley ook een dergelijke berekening uitgevoerd, waarin zelfconsistentie in feite werd meegenomen tot in een hogere orde dan in het geval van de één-dimensionale modelhalfgeleider, en ook in dat geval werd een goede compensatie gevonden. In dit proefschrift hebben we op grond van deze aanwijzingen voor de prototypische halfgeleider silicium en isolator diamant precies berekend wat de bijdrage tot de bandgap is van de laagste orde diagrammen verwaarloosd in de *GW*-theorie. Ook hiervoor hebben we het bovengenoemde plasmon-pool model gebruikt voor de energieafhankelijkheid van W . Het resultaat is dat er, tegen onze verwachting in, wel degelijk een niet verwaarloosbare bijdrage is tot de bandgap. Daarmee ligt de verklaring van het succes van de *GW*-theorie voor deze materialen nog open. Op grond van de bovengenoemde berekening aan het homogene elektron gas door Shirley (waarin zelfconsistentie dus wordt meegenomen tot in een hogere orde dan in onze berekeningen voor silicium en diamant), is de volgende stap wellicht in dit recept van Shirley te zoeken. Ons resultaat maakt in ieder geval duidelijk dat er absoluut geen sprake is van een eenvoudige convergentie.

Summary

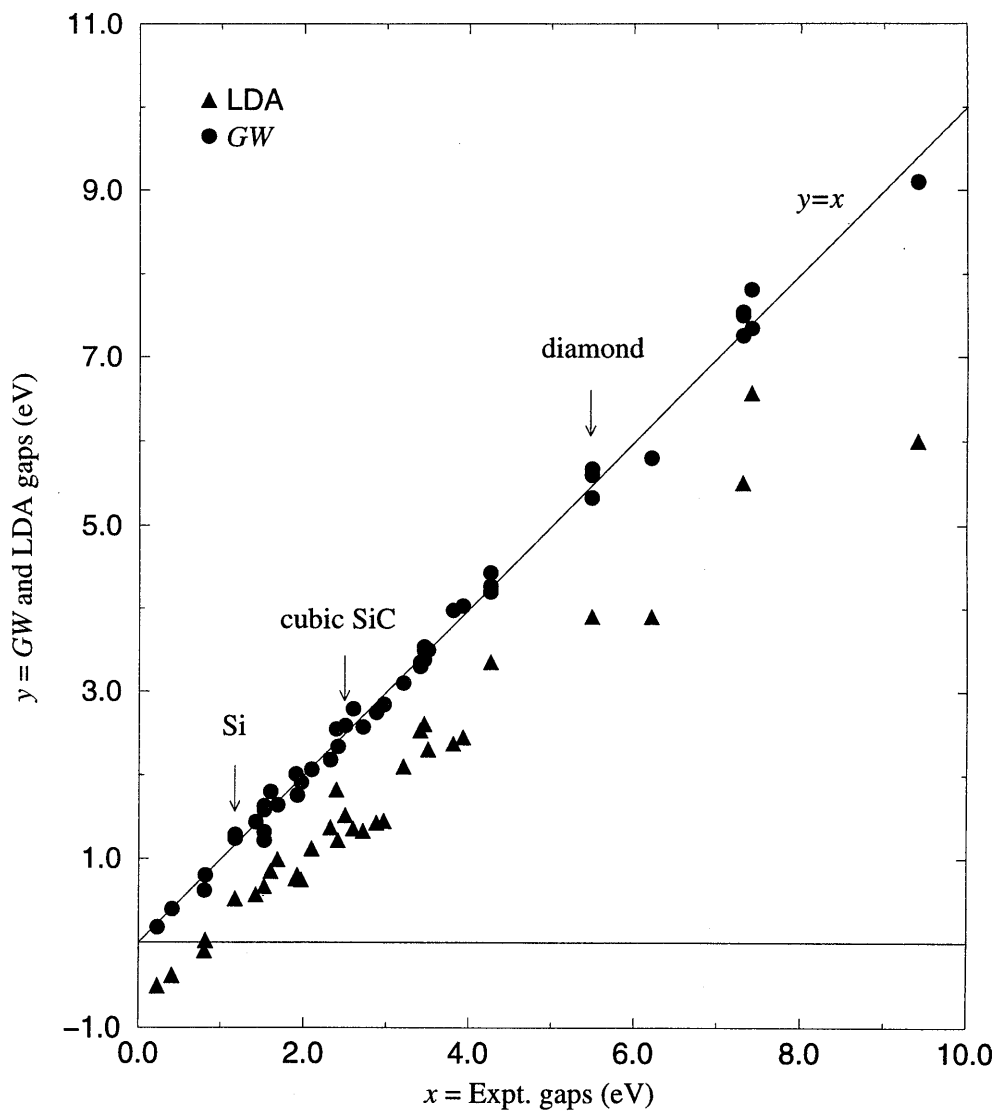
The so-called GW theory, which was formulated in the sixties, gives a quantum-mechanical description of excited electron states in a system with interacting electrons. Since the end of the eighties it has become clear that the GW theory provides a surprisingly good framework for calculating band structures. In particular, the electron energy bands around the band gap, i.e., the gap between the electron energies of the occupied electron states in the ground state of the system under consideration and the excited electron states, calculated within this framework, lead to excellent agreement with experimental data for a large group of semiconductors. Earlier schemes, such as the Hartree and the Hartree-Fock scheme, do not lead to agreement at all. Also the density-functional theory, despite its successful description of the ground-state properties of semiconductors, does not lead to satisfying results for the band structure around the band gap in the case of semiconductors.

In this thesis it is firstly investigated whether the GW theory also leads to good results if it is applied to three polytypes of silicon carbide, namely 2H, 4H, and 6H silicon carbide, semiconductors with 4, 8, and 12 atoms in the primitive unit cell, respectively. We show that the GW theory leads to excellent agreement with experiment also for these relatively complex semiconductors. It has to be remarked that in the employed algorithm we used a plasmon pole model that provides an analytical approximation for the energy dependence of the dynamically screened interaction W . So, it can be concluded that the GW theory, in connection with this plasmon pole model, leads to excellent agreement with experiment even for these complex semiconductors.

Secondly, this thesis focuses on the question why the GW theory apparently is so successful. In this connection, the leading idea is that in this theory the essential contribution to the electron energies is obtained by cutting off a perturbation series in terms of W to the lowest order. This perturbation series follows from a theory in which the total effect of the electron-electron interaction on the electron energies can be represented as an infinite sum of so-called Feynman diagrams. Hence, in the GW theory the higher-order diagrams are neglected. However, the convergence properties of the perturbation series are not known *a priori*. Nevertheless, recent calculations for the case of the homogeneous electron gas by Shirley as well as for the case of a one-dimensional model semiconductor yielded only a minor contribution of the next diagrams in the perturbation series. More precisely: for the one-dimensional model semiconductor the lowest order diagrams were calculated which contain so-called “self-consistency” and “vertex correction” contributions, and it was found that they compensate each other to a high degree. For the homogeneous electron gas a similar calculation was performed by Shirley, in which self-consistency in fact was carried through to higher order than in the case of the one-dimensional model semiconductor,

and also in that case a good compensation was found. On the basis of these indications, we have accurately calculated in this thesis the size of the contribution to the band gap from the lowest order diagrams that are neglected in the GW theory, for the prototypic semiconductor silicon and insulator diamond. Again we have used the above-mentioned plasmon pole model for the energy dependence of W . The result is that, contrary to our expectation, there is a relatively large contribution to the band gap of silicon and diamond. With that the success of the GW theory for these materials is still unexplained. On the basis of the above-mentioned calculation in the case of the homogeneous electron gas by Shirley (in which self-consistency has been carried through to higher order than in our calculations for silicon and diamond), the next step may be found in this recipe of Shirley. Anyway, our results make clear that it is not a matter of a simple convergence.

Figure 1.1: GW and LDA gaps versus the experimental gaps (in eV) for the set of semiconductors listed in Table 1.1.



Chapter 1:

Introduction

This thesis is devoted to the theory of excited states in semiconductors. More specifically, it focuses on the so-called *GW* theory, which has been proved to be successful in, among other things, predicting the energy-gap values of a large group of semiconductors. The energy gap, or (band) gap, being one of the most important characteristics of a semiconductor, is defined as the minimum energy required to remove an electron from the ground state of the semiconducting crystal and to promote it into an excited state. Metals can be said to have an energy gap equal to zero; they are good conductors of electrical current. Insulators, such as diamond, have large energy gaps, such that their conductivity is bad. The conductivity of a semiconductor lies in between that of metals and insulators, which explains the name semiconductor. Its energy gap is such that the (temperature-dependent) conductivity is generally much smaller than that of a metal. Semiconductors are of utmost technological importance. Applications range from single-circuit elements such as switches, diodes, transistors, and photo-detectors to modern electronic devices such as lasers (used in, for instance, optical communication) and computers.

In discussing semiconductors we restrict ourselves to crystalline materials in which the atoms are ordered periodically. The structure of the constituting individual atoms is well described by quantum mechanics in terms of negatively charged electrons moving in orbitals around a positively charged nucleus. When these atoms are brought together in a crystal, the outer orbitals of the atoms overlap and transform into energy bands. In semiconductors the energy gap separates occupied and unoccupied energy levels. In conventional theory one distinguishes valence and conduction bands for individual electrons. In this connection the energy gap is defined by the energy difference between the highest valence band and the lowest conduction band. If these two extrema are located at the same wave vector (characterizing the corresponding one-electron wave function) the gap is called a direct gap. If the corresponding wave vectors are different, the gap is called indirect. The so-called fundamental gap is defined as the minimum gap, which may be indirect.

From a fundamental point of view, the electronic system formed by a semiconductor is a many-body system with mutual Coulomb interaction between the electrons. It is therefore not at all obvious that a picture in which independent electrons move in a one-electron potential field leads to a valid description. One is in fact faced with the problem of solving Schrödinger's equation for many particles. Due to the mutual interaction it is not allowed to separate Schrödinger's equation into one-particle equations for independent electrons. In spite of this, one-particle schemes have been developed in the past in which it is attempted to construct effective potentials simulating, among other things, the mutual Coulomb interaction. Important historical steps in this connection are the proposals of Hartree, Slater, and Fock. In 1928 Hartree[43] suggested to introduce an effective potential felt by individual electrons due to the average charge distribution of all the other electrons plus the nuclei. Since the electrons are fermions and therefore obey the Pauli exclusion principle, the total wave function of the system must be antisymmetric under the interchange of two coordinates. This condition is not fulfilled by the Hartree wave function. In 1930 Slater[77] and Fock[30] proposed to take also the antisymmetry requirement for electrons into account, leading to the well-known Hartree-Fock (HF) scheme. In both the Hartree and the HF scheme the one-electron Schrödinger equations have to be solved iteratively.

In 1964 Hohenberg and Kohn developed the density-functional theory (DFT), which in principle gives an exact description of the ground-state properties by including the so-called exchange and correlation effects through an effective potential that is a functional of the ground-state electron density[46]. Practical application of DFT usually relies on the local-density approximation (LDA). Unfortunately, the DFT-LDA predicts energy gaps for semiconductors that are too small compared with experiment. It should be said that this is not in conflict with the exact character of DFT applicable to the ground state.

In 1965 Hedin developed a general quantum-mechanical scheme which describes excited-state properties through a so-called electron self-energy Σ . [44] From it, the so-called *GW* theory is derived, which is based on an approximation of Σ . The Hedin scheme and the *GW* approximation are given in Chapter 2.

1.1 The success of the *GW* theory

In recent years it has become clear that the *GW* approach gives excellent predictions of energy-gap values for semiconductors[44]. *GW* calculations appear to lead to energy gaps that are in excellent agreement with experiment for a large group of semiconductors. It has to be remarked that these *GW* calculations are based on two approximations to the extensive theory, called Hedin's scheme which exists of a set of coupled integral equations: The first approximation is that the so-called vertex corrections are omitted.

Table 1.1: Fundamental *GW* gaps as well as the LDA and experimental values (in eV) for a set of semiconductors ordered according to increasing experimental fundamental energy-gap value. The listed semiconductors have cubic symmetry, with the exception of the ones indicated with α which have wurtzite symmetry.

Material	LDA	<i>GW</i>	Expt.	Material	LDA	<i>GW</i>	Expt.
InSb	-0.51	0.18	0.23	GaP	1.82	2.55	2.39
InAs	-0.39	0.40	0.41	SiC	1.22	2.34, 2.37	2.41
Ge	≈ 0	0.75, 0.65	0.744	AlP	1.52	2.59	2.50
GaSb	-0.10	0.62	0.80	ZnTe	1.33	2.57	2.71
Si	0.52	1.29, 1.24	1.17	ZnSe α	1.43	2.75	2.87
InP	0.57	1.44	1.42	ZnSe	1.45	2.84	2.96
GaAs	0.67	1.22, 1.63	1.52, 1.63	GaN	2.1	3.1	3.2, 3.3
CdTe α	0.85	1.80	1.60	GaN α	2.3	3.5	3.5
AlSb	0.99	1.64	1.68	ZnS	2.37	3.98	3.80
CdSe	0.76	2.01	1.90	ZnS α	2.45	4.03	3.92
CdTe	0.80	1.76	1.92	diamond	3.90	5.6, 5.33	5.48
CdSe α	0.75	1.91	1.97	AlN	3.9	5.8	6.2
AlAs	1.37	2.18, 2.09	2.32, 2.24	LiCl	6.0	9.1	9.4

The second approximation is that only a first iteration *GW* result is being used instead of a so-called self-consistent one. The apparent success of this *GW* approach is demonstrated in Fig. 1.1 and Table 1.1. Here we have confronted the *GW*-obtained energy-gap values of 26 semiconductors with the experimental values [8, 61, 62]. The former values have been collected from Refs. [1],[5],[34],[35],[48], [49], [73], [74], and [85]. It is observed both from Table 1.1 and Fig. 1.1 that the difference between experimentally obtained and *GW*-obtained energy-gap values is at most a few tenth of an eV. This extremely good result is apparently independent of the absolute energy-gap values of the involved semiconductors. We have included in Table 1.1 and Fig. 1.1 the DFT-LDA-obtained values as well. It is clearly seen that the latter energy-gap values are systematically too small when compared with the experimental values. There seems to be no doubt whatsoever that *GW* theory is capable of predicting energy-gap values of a large group of semiconductors. However, the question is whether this also holds true if we apply this theory to more complicated semiconductors (i.e., with larger primitive unit cells), such as the various polytypes of silicon carbide (SiC). This is one of the questions addressed in this thesis. In one of the following chapters (Chapter 3) it will be shown that also in these cases the *GW* approach

is successful.

1.2 Why is the GW theory so successful?

The remaining question now is why the GW approach is successful. In Chapter 4 we describe an attempt to deal with this question by focusing on those contributions to the energy gap that have been intentionally left out in the GW approach: the so-called higher-order corrections. Investigation of these corrections is computationally very costly for semiconductors, implying that we have to restrict ourselves to the first-order corrections. It is, however, by no means clear *a priori* that the sum of this restricted group of corrections will lead to a vanishing contribution to the energy gap. The reason that we nevertheless put effort in the calculation of these first-order contributions, which we will perform for the prototypical semiconductor Si and insulator diamond, lies in the circumstance that such calculations have already been performed for simpler systems such as (1) the homogeneous electron gas[76] and (2) the case of a quasi-one-dimensional semiconducting wire[37]. It was shown in both cases that the so-called lowest-order vertex (V) and self-consistency (SC) corrections, i.e., the corrections to GW under consideration, have the tendency to compensate each other to a high degree. In a recent study, Shirley[76] reported on a calculation for the homogeneous electron gas case in which GW was considered together with its lowest-order V correction, the difference with earlier calculations being that both were brought very close to self-consistency. The resulting bandwidth, i.e., the width of the occupied energy levels, was found to be very close to the GW value. For the case of the quasi-one-dimensional semiconducting wire de Groot *et al.*[37] reported that the resulting energy gap of a calculation in which all first-order corrections to GW have been included is very close to the GW energy gap. In view of all these results it is of interest to know how good the compensation of the respective additional contributions will be in the case of real systems such as Si and diamond. As mentioned above, this question is addressed in Chapter 4. It is an extension to real systems of the work reported on in Ref. [37].

In order to facilitate the reading of Chapters 3 and 4, both of which have been published in the open literature, we first give an introductory sketch of the general theory, in Chapter 2. We start by giving the many-electron Hamiltonian, after which follows a short description of DFT, DFT-LDA, Green's function theory and quasiparticle theory, Hedin's scheme expressed both in formulae and in terms of Feynman diagrams, and, finally, of the GW approach and its higher-order corrections. In the introductions of Chapters 3 and 4 we will also pay attention to extensive historical reviews. As mentioned before, the GW approach will be shown to be successful for three polytypes of SiC; this is described in Chapter 3. The higher-order corrections, as calculated in Chapter 4, leave us with the puzzling result that the compensation between the higher-order corrections, if any, is clearly insufficient

in order to “explain” the success of the celebrated *GW* theory. It is suggested in Chapter 4 that possibly Shirley’s recipe could give the answer. However, such a “full” calculation of the required terms seems to be beyond present reach for real semiconductors. It will have to wait for either more computing power or more refined calculational schemes.

Chapter 2:

Theory

2.1 Introduction

This Chapter is devoted to the introduction of the key elements in the theory describing the electronic behaviour of semiconductors, especially the treatment of the excited electron states. To this end we start in Section 2.2 by giving the Hamiltonian of the many-electron system as valid for a semiconductor. In Section 2.3 the density-functional theory (DFT) is briefly introduced; the well-known Kohn-Sham equations will be given. DFT in the local-density approximation (LDA) has made it possible to introduce a special effective potential v^{eff} felt by every electron. It has been shown in a large number of cases that DFT-LDA is very successful in describing ground-state properties; see, for instance, Ref. [52]. It is, however, incapable of correctly treating excited states and leads to, e.g., incorrect predictions for energy gaps in semiconductors. A correct treatment is given by the so-called *GW* theory, in which the above effective potential $v^{\text{eff}}(\vec{r})$ is replaced by a nonlocal, time-dependent self-energy operator. *GW* theory has been applied with success to a number of semiconductors. The time-dependent self-energy leads to a picture in which excitations have finite lifetimes: the so-called quasiparticles, which are introduced in Section 2.4. Subsections 2.4.1 — 2.4.3 deal with the general characteristics of the Green's function theory in which both the self-energy operator and the quasiparticle concept play dominant roles. Subsection 2.4.4 focuses on the *GW* approach. Its description can be viewed upon as introductory to Chapter 3 in which the method is applied to some polytypes of SiC. Subsection 2.4.5 is a short introduction to Chapter 4 in which an attempt is made to contribute to the understanding of the apparent success of the *GW* approach.

2.2 The Hamiltonian of the many-electron system

In describing the properties of a many-electron system with mutual interactions between the electrons, it is helpful to make use of the second-quantization formalism or, rather, occupation number formalism.[21, 29, 66] This is a formulation of quantum mechanics that explicitly accounts for, in the case of electrons, the antisymmetry requirement of wave functions. We make use of electron creation and annihilation operators, denoted by $\psi^\dagger(\vec{r}, t)$ and $\psi(\vec{r}, t)$, respectively. These operators create or annihilate an electron at a given space-time point \vec{r}, t . They obey the relations (spin indices are omitted)

$$[\psi^\dagger(\vec{r}_1, t), \psi^\dagger(\vec{r}_2, t)]_+ = [\psi(\vec{r}_1, t), \psi(\vec{r}_2, t)]_+ = 0, \quad (2.1)$$

$$[\psi(\vec{r}_1, t), \psi^\dagger(\vec{r}_2, t)]_+ = \delta(\vec{r}_1 - \vec{r}_2), \quad (2.2)$$

in which $[A, B]_+ \equiv AB + BA$ is the anti-commutation operation. The complete Hamiltonian H of a many-electron system is given by

$$H = T + U + V, \quad (2.3)$$

$$T = -\frac{\hbar^2}{2m_e} \int d^3r \psi^\dagger(\vec{r}) \nabla^2 \psi(\vec{r}), \quad (2.4)$$

$$U = \int d^3r \psi^\dagger(\vec{r}) u(\vec{r}) \psi(\vec{r}), \quad (2.5)$$

$$V = \frac{1}{2} \int \int d^3r d^3r' \psi^\dagger(\vec{r}) \psi^\dagger(\vec{r}') v(\vec{r} - \vec{r}') \psi(\vec{r}') \psi(\vec{r}), \quad (2.6)$$

where

$$\psi(\vec{r}) = e^{-iHt/\hbar} \psi(\vec{r}, t) e^{iHt/\hbar}. \quad (2.7)$$

T is the kinetic energy operator. m_e is the electron mass. U is the external potential operator: $u(\vec{r}) = u(\vec{r} + \vec{R})$ is the periodic external potential felt by each electron (\vec{R} is a lattice vector). In $u(\vec{r})$ we include the potential caused by the periodically arranged nuclei plus the innermost unaffected electrons, also called core electrons. In this approximation the outer electrons, which are subdivided into valence and conduction electrons, feel the combined field of the ion cores, defined as the nuclei plus the core electrons. Throughout this thesis it is assumed that the effect of the ion cores in the theory can be described by means of pseudopotentials felt by the outer electrons. This circumvents the need for an all-electron description. In combination with the periodicity of the crystal the ion pseudopotential approach allows efficient use of a plane wave basis set, reducing the size of the Hamiltonian matrix. Furthermore, a plane wave formalism is one of the simplest formalisms to implement numerically. In Eq. (2.3), V is the interaction operator between the electrons, interacting through the Coulomb interaction v :

$$v(i, j) = v(\vec{r}_i - \vec{r}_j) \delta(t_i - t_j) = \frac{e^2}{4\pi\epsilon_0 |\vec{r}_i - \vec{r}_j|} \delta(t_i - t_j). \quad (2.8)$$

Here we have introduced a short-hand notation j for the space-time point \vec{r}_j, t_j . e is the electron charge and ϵ_0 is the vacuum permittivity. The treatment of V is the central issue in the many-electron problem. One may, e.g., try to simulate the effects of V by constructing an effective potential $v^{\text{eff}}(\vec{r})$ and rewriting H as follows:

$$H = H_0 + H_1, \quad (2.9)$$

with

$$H_0 \equiv T + U + V^{\text{eff}}, \quad (2.10)$$

$$H_1 \equiv V - V^{\text{eff}}, \quad (2.11)$$

$$V^{\text{eff}} = \int d^3r \psi^\dagger(\vec{r}) v^{\text{eff}}(\vec{r}) \psi(\vec{r}). \quad (2.12)$$

The usefulness of introducing such a v^{eff} lies in the possibility to reduce the relative importance of the perturbing part H_1 in H . In Subsection 2.3 we describe a choice for v^{eff} made within DFT.

2.3 Density-functional theory

In this Section we give a very brief description of an effective potential v^{eff} which turns out to give an excellent description of the ground-state properties of a solid. The density-functional theory (DFT) in which this potential has its origin, has been developed by Hohenberg and Kohn.[46] In 1964 Hohenberg and Kohn[46] proved that (1) the ground state of a many-electron system is a unique functional of its ground-state electron density $\rho(\vec{r})$ and that (2) the ground-state energy has its minimum value for the exact $\rho(\vec{r})$. In the theory of Kohn and Sham, see Ref. [59], the interacting many-electron system is replaced by a fictitious noninteracting system having the same density and the proper $\rho(\vec{r})$ can be obtained by solving the equations

$$\left(-\frac{\hbar^2}{2m_e} \nabla^2 + u(\vec{r}) + v^{\text{eff}}[\rho(\vec{r})] \right) \phi_i(\vec{r}) = \varepsilon_i \phi_i(\vec{r}),$$

$$\rho(\vec{r}) = \sum_{i=1}^N |\phi_i(\vec{r})|^2, \quad (2.13)$$

where $\{\phi_i\}$ are orthonormal eigenfunctions and $\{\varepsilon_i\}$ the associated eigenvalues. The sum in Eq. (2.13) extends over the N occupied eigenstates. These states are each at least doubly degenerate, since spin-up and spin-down electrons are assumed to have the same energy. In the noninteracting system, the electrons move in an effective potential

$$v^{\text{eff}}(\vec{r}) = v^{\text{H}}(\vec{r}) + v^{\text{XC}}(\vec{r}). \quad (2.14)$$

Here the Hartree potential $v^H(\vec{r})$ reads:

$$v^H(\vec{r}) = \int d^3r' v(\vec{r} - \vec{r}')\rho(\vec{r}'), \quad (2.15)$$

while the exchange-correlation potential v^{XC} is given by

$$v^{XC}(\vec{r}) = \left. \frac{\delta E^{XC}[\rho]}{\delta \rho} \right|_{\rho=\rho(\vec{r})}, \quad (2.16)$$

where E^{XC} is the exchange-correlation-energy functional and the square brackets indicate functional dependence. In Eq. (2.16), $\delta E^{XC}/\delta \rho$ means that we must take the functional derivative of E^{XC} with respect to ρ .

Within the local-density approximation (LDA) of DFT, E^{XC} is given by

$$E^{XC}[\rho] = \int d^3r \rho(\vec{r})\varepsilon^{XC}(\rho(\vec{r})), \quad (2.17)$$

where ε^{XC} is the exchange-correlation energy per electron of the homogeneous electron gas. A variety of approximations exists for the correlation part of ε^{XC} . A practical approximation is the Wigner interpolation formula[83] which leads to the following expression for ε^{XC} :

$$\varepsilon^{XC}(\rho) = -\frac{e^2}{4\pi\epsilon_0} \left[\frac{3}{4} \left(\frac{9}{4\pi^2} \right)^{1/3} \frac{1}{r_s} + \frac{0.44}{(7.8a_0 + r_s)} \right], \quad (2.18)$$

where $\frac{4}{3}\pi r_s^3 = \rho^{-1}$ and a_0 is the Bohr radius of 0.529177 Å.

Formally, the eigenvalues ε_i in the Kohn-Sham Eqs. (2.13) have no physical interpretation. Nevertheless, they are often interpreted as excitation energies. However, the Kohn-Sham eigenvalues belonging to unoccupied electron states are generally quite different from experimentally obtained energy levels of unoccupied states. The LDA substantially underestimates, e.g., the fundamental gap E_g for a large number of semiconductors; see Table 1.1.

2.4 Quasiparticle theory

According to common practice, elementary excitations of a many-electron system are classified into two categories: particle-like and collective excitations.[66] One can imagine injecting a particle with a particular momentum and energy into (or removing one from) the system and observing how the system reacts in space and time. We speak of a quasiparticle if the particle plus its cloud of disturbance is sufficiently long-lived. An excitation that involves a collective, wavelike motion of the electrons in the system is called a plasmon.

2.4.1 Green's function theory

The quantum-mechanical treatment of many-electron systems with mutual interaction between the electrons is very conveniently expressed in terms of Green's functions. The (zero-temperature) one-electron Green's function is defined as the expectation value in the many-electron ground state of a time-ordered product of a creation and an annihilation operator (multiplied by $-i$) [29]:

$$G(1, 2) = -i\langle N | \mathcal{T} \{ \psi(1) \psi^\dagger(2) \} | N \rangle. \quad (2.19)$$

The normalized time-independent ground state of the system of N interacting electrons is denoted by $|N\rangle$. The Wick time-ordering operator \mathcal{T} is defined as

$$\mathcal{T} \{ \psi(1) \psi^\dagger(2) \} = \begin{cases} \psi(1) \psi^\dagger(2) & \text{if } t_1 > t_2, \\ -\psi^\dagger(2) \psi(1) & \text{if } t_2 > t_1. \end{cases} \quad (2.20)$$

The one-electron Green's function $G(1, 2)$ describes for $t_1 > t_2$ the motion of an added electron from \vec{r}_2, t_2 to \vec{r}_1, t_1 , whereas for $t_2 > t_1$ it describes the motion of an added hole from \vec{r}_1, t_1 to \vec{r}_2, t_2 , in an N -electron system.

Starting from the Heisenberg equation of motion,

$$i\hbar \frac{\partial}{\partial t} \psi^{(\dagger)}(\vec{r}, t) = [\psi^{(\dagger)}(\vec{r}, t), H]_-, \quad (2.21)$$

where $[A, B]_- \equiv AB - BA$ is the commutation operation, it can be shown that the Green's function $G(1, 2)$ of Eq. (2.19) satisfies the following basic equation of the Green type:

$$\left[i\hbar \frac{\partial}{\partial t_1} + \frac{\hbar^2}{2m_e} \nabla_1^2 - u(\vec{r}_1) - v^H(\vec{r}_1) \right] G(1, 2) - \hbar \int d(3) \Sigma(1, 3) G(3, 2) = \hbar \delta(1, 2). \quad (2.22)$$

Eq. (2.22) is a formal defining equation for the so-called electron self-energy operator Σ . Σ contains all the exchange-correlation effects of the electrons. If we approximate these effects by means of the local function $v^{XC}(\vec{r})$ of DFT-LDA, the function $\hbar \Sigma(1, 3)$ reduces to $v^{XC}(\vec{r}_1) \delta(1, 3)$, and the Green's function G reduces to the LDA Green's function G^0 :

$$\left[i\hbar \frac{\partial}{\partial t_1} + \frac{\hbar^2}{2m_e} \nabla_1^2 - u(\vec{r}_1) - v^{\text{eff}}(\vec{r}_1) \right] G^0(1, 2) = \hbar \delta(1, 2). \quad (2.23)$$

Combining Eqs. (2.22) and (2.23) one can derive the Dyson equation

$$G(1, 2) = G^0(1, 2) + \int d(3, 4) G^0(1, 3) \left[\Sigma(3, 4) - \hbar^{-1} v^{XC}(\vec{r}_3) \delta(3, 4) \right] G(4, 2). \quad (2.24)$$

How the quasiparticle band structure can be related to the self-energy Σ is treated in Subsection 2.4.3.

2.4.2 Hedin's scheme

Hedin developed a scheme to calculate the self-energy Σ , based on linear response theory.[44] He derived a set of five coupled integral equations, namely the Dyson equation for the electron Green's function G [Eq. (2.24)] together with four additional equations, reading:

$$\Sigma(1, 2) = \frac{i}{\hbar} \int d(3, 4) G(1, 3) W(1^+, 4) \Gamma(3, 2; 4), \quad (2.25)$$

$$W(1, 2) = v(1, 2) + \int d(3, 4) v(1^+, 3) P(3, 4) W(4, 2), \quad (2.26)$$

$$P(1, 2) = -\frac{2i}{\hbar} \int d(3, 4) G(1, 3) G(4, 1^+) \Gamma(3, 4; 2), \quad (2.27)$$

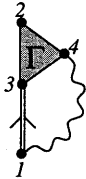
$$\begin{aligned} \Gamma(1, 2; 3) &= \delta(1, 2) \delta(1, 3) + \\ &\int d(4, 5, 6, 7) \frac{\delta \Sigma(1, 2)}{\delta G(4, 5)} G(4, 6) G(7, 5) \Gamma(6, 7; 3). \end{aligned} \quad (2.28)$$

The superscript $+$ in 1^+ means that we must increment the time variable t_1 by an infinitesimally small amount η . The factor of 2 in Eq. (2.27) is due to spin summation. Three additional functions occurring in these equations are the dynamically screened interaction W , the polarizability P , and the so-called vertex function Γ . As can be seen from Eq. (2.25), the self-energy Σ depends both explicitly and implicitly on G .

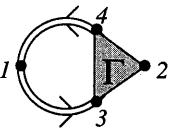
The Dyson equation and the Hedin equations can be represented in diagrammatic language. In the diagrammatic equations, see Eqs. (2.29) — (2.33), the solid directed line denotes the LDA Green's function G^0 , the solid directed double line denotes the Green's function G , the dotted line denotes the bare Coulomb interaction v , the wiggly line denotes the dynamically screened interaction W , and the cross denotes minus the LDA exchange-correlation potential. The resulting diagrams obey well-defined calculational rules[66] by means of which their contributions can in principle be determined.

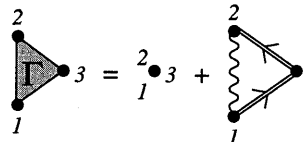
$$G(1,2) = 1 \Rightarrow 2$$

$$= 1 \rightarrow 2 + 1 \rightarrow 3 \text{---} \Sigma \text{---} 4 \Rightarrow 2 + 1 \rightarrow \frac{3}{4} \Rightarrow 2 \quad (2.29)$$

$$\Sigma(1,2) = 1 \text{---} \Sigma \text{---} 2 = 3 \text{---} \Gamma \text{---} 4$$

(2.30)

$$W(1,2) = 1 \text{---} 2 = 1 \text{---} 2 + 1 \text{---} 3 \text{---} P \text{---} 4 \text{---} 2 \quad (2.31)$$

$$P(1,2) = 1 \text{---} P \text{---} 2 = 1 \text{---} \Gamma \text{---} 3 \text{---} 4 \text{---} 1$$

(2.32)

$$\Gamma(1,2;3) = \Gamma \text{---} 3 = \frac{2}{1} \text{---} 3 + \text{higher order in } W$$

(2.33)

2.4.3 Quasiparticle band structure

In band structure theory wave functions are labeled with a band index l and a wave vector \mathbf{k} . To each wave function or state $|l, \mathbf{k}\rangle$ corresponds an energy $E_l(\mathbf{k})$. The whole of curves $E_l(\mathbf{k})$ is called the band structure of the solid under consideration.

In order to relate the Green's function G to wave functions and energies we first define the Fourier transform of G with respect to time by

$$G(\vec{r}_1, \vec{r}_2; \varepsilon) = \int d(t_1 - t_2) G(1, 2) e^{i\varepsilon(t_1 - t_2)/\hbar}. \quad (2.34)$$

It has generally been proved that the Green's function G of Eq. (2.22) can be written as [26]

$$G(\vec{r}_1, \vec{r}_2; \varepsilon) = \hbar \sum_{l, \mathbf{k}} \frac{\psi_{l, \mathbf{k}}(\vec{r}_1; \varepsilon) \psi_{l, -\mathbf{k}}(\vec{r}_2; \varepsilon)}{\varepsilon - E_l(\mathbf{k}; \varepsilon) + i\eta \operatorname{sgn}[\operatorname{Re}\{E_l(\mathbf{k}; \varepsilon)\} - \mu]}, \quad (2.35)$$

where μ is the chemical potential which in the case of a semiconductor is situated in the energy gap and where the wave functions $\psi_{l, \mathbf{k}}(\vec{r}; \varepsilon)$ fulfill the equation

$$\left[E_l(\mathbf{k}; \varepsilon) + \frac{\hbar^2}{2m} \nabla^2 - u(\vec{r}) - v^H(\vec{r}) \right] \psi_{l, \mathbf{k}}(\vec{r}; \varepsilon) - \hbar \int d^3 r' \Sigma(\vec{r}, \vec{r}'; \varepsilon) \psi_{l, \mathbf{k}}(\vec{r}'; \varepsilon) = 0. \quad (2.36)$$

Expanding the wave functions $\psi_{l, \mathbf{k}}(\vec{r}; \varepsilon)$ into plane waves:

$$\psi_{l, \mathbf{k}}(\vec{r}; \varepsilon) = \frac{1}{\sqrt{\Omega}} \sum_{\mathbf{G}} d_{l, \mathbf{k}}(\mathbf{G}; \varepsilon) e^{i(\mathbf{k} + \mathbf{G}) \cdot \vec{r}}, \quad (2.37)$$

where \mathbf{G} is a reciprocal lattice vector and Ω is the crystal volume, and Fourier transforming Eq. (2.35) with respect to the space variables,

$$G_{\mathbf{G}, \mathbf{G}'}(\mathbf{k}; \varepsilon) = \frac{1}{\Omega} \int d^3 r_1 \int d^3 r_2 e^{-i(\mathbf{k} + \mathbf{G}) \cdot \vec{r}_1} G(\vec{r}_1, \vec{r}_2; \varepsilon) e^{i(\mathbf{k} + \mathbf{G}') \cdot \vec{r}_2}, \quad (2.38)$$

one obtains

$$G_{\mathbf{G}, \mathbf{G}'}(\mathbf{k}; \varepsilon) = \hbar \sum_l \frac{d_{l, \mathbf{k}}(\mathbf{G}; \varepsilon) d_{l, \mathbf{k}}^*(\mathbf{G}'; \varepsilon)}{\varepsilon - E_l(\mathbf{k}; \varepsilon) + i\eta \operatorname{sgn}[\operatorname{Re}\{E_l(\mathbf{k}; \varepsilon)\} - \mu]}. \quad (2.39)$$

Thusfar no approximations for the Green's function G have been made. The so-called quasiparticle approximation follows if it is assumed that the function G of Eq. (2.39) has simple poles at the quasiparticle energies $E_l(\mathbf{k}) \equiv E_l(\mathbf{k}; E_l(\mathbf{k}))$. The (possible) singularities due to the non-analyticity of $d_{l, \mathbf{k}}(\mathbf{G}; \varepsilon)$ or $E_l(\mathbf{k}; \varepsilon)$ will be disregarded. The corresponding quasiparticle approximation of G is then obtained by putting

$$G_{\mathbf{G}, \mathbf{G}'}(\mathbf{k}; \varepsilon) \approx \hbar \sum_l g_{l, \mathbf{k}} \frac{d_{l, \mathbf{k}}(\mathbf{G}) d_{l, \mathbf{k}}^*(\mathbf{G}')}{\varepsilon - E_l(\mathbf{k}) + i\eta \operatorname{sgn}[\operatorname{Re}\{E_l(\mathbf{k})\} - \mu]}, \quad (2.40)$$

with

$$g_{l,\mathbf{k}} = \left(1 - \frac{\partial E_l(\mathbf{k}; \varepsilon)}{\partial \varepsilon} \Big|_{\varepsilon = E_l(\mathbf{k})} \right)^{-1}, \quad (2.41)$$

where $g_{l,\mathbf{k}}$ is the wave-function renormalization factor. The corresponding quasiparticle band structure equation, with which $d_{l,\mathbf{k}}(\mathbf{G})$ and $E_l(\mathbf{k})$ can be obtained, reads:

$$\left[\frac{\hbar^2}{2m} (\mathbf{k} + \mathbf{G})^2 - E_l(\mathbf{k}) \right] d_{l,\mathbf{k}}(\mathbf{G}) + \sum_{\mathbf{G}'} \left[u_{\mathbf{G},\mathbf{G}'} + v_{\mathbf{G},\mathbf{G}'}^{\text{H}}(\mathbf{k}) + \hbar \Sigma_{\mathbf{G},\mathbf{G}'}(\mathbf{k}; E_l(\mathbf{k})) \right] d_{l,\mathbf{k}}(\mathbf{G}') = 0, \quad (2.42)$$

where the Fourier transform with respect to the space variables has been applied; $\Sigma_{\mathbf{G},\mathbf{G}'}(\mathbf{k}; \varepsilon)$, for instance, is the Fourier transform of the self-energy. Generally, Σ is non-Hermitian and therefore the resulting eigenvalues $E_l(\mathbf{k})$ of Eq. (2.42) can be complex.

2.4.4 The *GW* approach

By approximating the vertex function $\Gamma(1, 2; 3)$ of Eq. (2.28) by $\delta(1, 2)\delta(1, 3)$, the first-order expansion of Σ and zeroth-order expansion of P in terms of W are obtained, to which we will refer as (Hedin's) *GW* approach. This leads to the following space-time expression of P , which is the so-called “random-phase approximation” (RPA) polarizability:

$$P^{\text{RPA}}(\vec{r}, \vec{r}'; t) = -2iG(\vec{r}, \vec{r}'; t)G(\vec{r}', \vec{r}, -t), \quad (2.43)$$

while the space-time expression for the *GW* self-energy Σ reads:

$$\Sigma^{\text{GW}}(\vec{r}, \vec{r}'; t) = iG(\vec{r}, \vec{r}'; t)W(\vec{r}, \vec{r}'; t). \quad (2.44)$$

The name “*GW*” is clear from Eq. (2.44). In most actual practice of *GW* calculations the Green's function G of Eq. (2.40) is further approximated by the noninteracting Green's function G^0 (i.e., the *GW* approach is applied non-self-consistently):

$$G_{\mathbf{G},\mathbf{G}'}^0(\mathbf{k}; \varepsilon) = \hbar \sum_l \frac{d_{l,\mathbf{k}}^0(\mathbf{G})d_{l,\mathbf{k}}^{0*}(\mathbf{G}')}{\varepsilon - \varepsilon_l(\mathbf{k}) + i\eta \operatorname{sgn}[\varepsilon_l(\mathbf{k}) - \mu]}, \quad (2.45)$$

where ε_l and d_l^0 are the energies and plane-wave coefficients, respectively, of the starting point wave functions obtained within the LDA. Concerning W , often a plasmon pole model (PPM) is employed that provides an analytical approximation for its energy dependence in order to facilitate the calculations; see, for instance, Refs. [50, 64, 73, 84]. The *GW* approach has already been proved to be of great practical importance for quite a number of substances. Moreover, by calculating an exchange-correlation potential from the *GW*

self-energy, it was shown in Ref. [35] that the interpretation of the one-electron DFT-LDA band structure as quasiparticle energies is not only invalid for the LDA, but is in fact inherent to DFT. More details on the GW approach can be found in a recent review article by Aryasetiawan and Gunnarsson[1].

In Chapter 3 we will apply the GW approach to three hexagonal polytypes of SiC, i.e. 2H, 4H, and 6H SiC, semiconductors with 4, 8, and 12 atoms in the primitive unit cell, respectively, in order to check whether the GW method also works for these rather complicated semiconductors. In this connection, we will make use of the PPM of Engel and Farid[25] in order to model the energy dependence of W . We will find that the GW method yields very good results for these SiC polytypes.

2.4.5 Higher-order corrections

In view of the apparent success of the GW theory in the case of semiconductors, also when applied to polytypes of SiC, the question arises where this success originates from. Obviously, the higher-order contributions to Σ and P not considered within GW will either have to cancel each other or will have to be small individually. Summation and actual calculation of the remaining diagrams has been out of the question thusfar; the convergence properties of the series of higher-order contributions, arranged in the order in W , are not clear. In the more simple system of the homogeneous electron gas[76] there are, however, indications that so-called self-consistency corrections and vertex corrections show the tendency of cancelling each other to a high degree. In the case of a quasi-one-dimensional model semiconductor[37] the cancellation effects are, in a way, more subtle. It was reported in Ref. [37] that the inclusion of the first-order corrections to both Σ and P leads only to a small change in the calculated quasiparticle gap of the quasi-one-dimensional model semiconductor, compared to its GW gap. Furthermore, it was shown that a relatively large change occurs if the first-order corrections are not added to P but only to Σ . In view of these results it is worthwhile to investigate whether such cancellations also occur in realistic systems such as the semiconductor Si and insulator diamond. Both a positive as well as a negative answer to the question whether such cancellations occur can be considered to be extremely helpful in the search for a better understanding of the success of GW .

In Chapter 4 we calculate the contributions to Σ due to all diagrams which are of second order in W . We also investigate the contributions to P which are of first order in W ; this "improved" P is furthermore used to calculate an "improved" W . Again we will use the PPM of Engel and Farid[25] for the energy dependence of W . For completeness it should be noted that, when considering Σ to second order in W , it is consistent to consider the second-order Hartree correction diagrams as well. This will be carried through in Chapter 4. However, the total contribution from the additional diagrams is very small due to the

fact that the LDA ground-state density is extremely close to the exact one. The result of our calculation in Chapter 4 for the semiconductor Si and insulator diamond is that the additional diagrams to P largely cancel each other, while the additional diagrams to Σ do not cancel each other to a sufficient degree. The latter is an intriguing and unexpected result.

Chapter 3:

Ab initio quasiparticle energies in 2H, 4H, and 6H SiC

Published in *R.T.M. Ummels, P.A. Bobbert, and W. van Haeringen, Phys. Rev. B* **58**, 6795 (1998).[79]

Abstract

Ab initio quasiparticle energies are calculated for the 2H, 4H, and 6H polytypes of SiC within the *GW* approximation for the self-energy. The starting point is a calculation within the pseudopotential local-density approximation framework. The calculated fundamental gaps of 3.15, 3.35, and 3.24 eV for 2H, 4H, and 6H SiC, respectively, show very good agreement with experimental data. The energy dependence of the screened interaction is modeled by a plasmon pole model from which the plasmon band structures are obtained.

3.1 Introduction

SiC polytypes are wide-band-gap indirect semiconductors with a relatively large variation in electronic band-gap magnitude, compared to other wide-band-gap materials such as the II-VI compounds ZnS and CdS. In 1964 Choyke *et al.*[17] found, covering seven polytypes of SiC excluding the 2H polytype, that the experimental fundamental band gap varies roughly linearly with the degree of hexagonal nature (h) for polytypes up to $h = 50\%$. It was recently shown[4, 7, 41] that this variation can be very well reproduced in a model that treats the polytypes as different stackings of mutually twisted cubic SiC layers with appropriate boundary conditions at the layer interfaces. The electronic structure of cubic (3C, or β) SiC is then taken as the starting point. The essential mechanism of the band-gap formation can be described within an even more simple Kronig-Penney-like model.[6, 7, 41]

Of course, a more fundamental treatment of the electronic structure should display the same band-gap variation. Indeed, calculations based on the local-density approximation (LDA) of density-functional theory (DFT) show such a variation; see Ref. [53] and references therein. However, the size of the LDA gaps is much too low due to a nowadays well-known deficiency of DFT[34], which is not in conflict, however, with the exact character of DFT applicable to the ground state. This deficiency can be cured by replacing the local and energy-independent exchange-correlation potential within DFT by a nonlocal energy-dependent self-energy obtained within the *GW* approximation.[1, 34, 35, 44, 49, 64] Such an approach was followed for the cubic polytype of SiC leading to excellent agreement with experiment.[5, 7, 73] Wenzien, Käckell, Bechstedt, and Cappellini[81] (WKBC) have performed simplified *GW* calculations for 3C, 2H, 4H, and 6H SiC. The simplifications involve the use of a model dielectric function and an approximate treatment of the so-called local-field effects. The resulting fundamental gaps, calculated at the theoretical lattice constants, show good agreement with experiment for 3C and 6H SiC, while the agreement is reasonable for 4H and 2H SiC: 3.68, 3.56, 3.25, and 2.59 eV for 2H, 4H, 6H, and 3C SiC, while experimental values are 3.33, 3.28, 3.10, and 2.42 eV, respectively. The latter values are absorption gaps[17, 68] that are, except for 2H SiC, corrected for measured exciton binding energies.[23, 75]

The aim of the present paper is to perform *GW* calculations for the 2H, 4H, and 6H SiC polytypes without the approximations made in Ref. [81] and to investigate whether possibly better agreement with experiment can be obtained. Since the fundamental band gaps of the crystals under consideration are accurately known experimentally, such an investigation can shed more light on the reliability of the *GW* method. For the energy dependence of the screened interaction appearing in the *GW* method we utilize a plasmon pole model (PPM), yielding as an interesting by-product the plasmon band structure, which can be subjected to experimental verification.[25] A previous application of this plasmon pole model to 3C SiC yielded quasiparticle energies and a lowest plasmon energy in excellent agreement with experiment.[5]

In Sec. 3.2 we will give a description of some theoretical and calculational details. In Sec. 3.3 we will give the results of the plasmon band structures and *GW* quasiparticle energies. For the latter results we have concentrated on energy levels around the band gap, at specific points in the first Brillouin zone (1BZ) of 2H, 4H, and 6H SiC; see Fig. 3.2. We conclude briefly in Sec. 3.4.

3.2 Theory

As input to our *GW* calculations we use wave functions and energies $|l, \mathbf{k}\rangle$ and $\varepsilon_l(\mathbf{k})$, respectively, obtained within the framework of the LDA. Here \mathbf{k} is a wave vector in the 1BZ

and l is an electron-band index. The closeness of the quasiparticle (QP) wave functions in the GW approximation and the LDA wave functions was demonstrated in various cases[35, 49] and we assume that the same is true in the present case, so that we can replace QP by LDA wave functions. Using a first-order expansion of the self-energy operator $\Sigma(\mathbf{k}; \varepsilon)$, where ε is the energy, around the LDA energies one finds for the QP energies

$$E_l^{\text{QP}}(\mathbf{k}) = \varepsilon_l(\mathbf{k}) + Z_{l,\mathbf{k}} \langle l, \mathbf{k} | -v^{\text{XC}} + \hbar \Sigma^{\text{X}}(\mathbf{k}) + \hbar \Sigma^{\text{C}}(\mathbf{k}; \varepsilon_l(\mathbf{k})) | l, \mathbf{k} \rangle, \quad (3.1)$$

where $Z_{l,\mathbf{k}}$ is the so-called wave-function renormalization factor, given by

$$Z_{l,\mathbf{k}} = \left(1 - \hbar \langle l, \mathbf{k} | \frac{\partial \Sigma^{\text{C}}(\mathbf{k}; \varepsilon)}{\partial \varepsilon} \Big|_{\varepsilon = \varepsilon_l(\mathbf{k})} | l, \mathbf{k} \rangle \right)^{-1}. \quad (3.2)$$

In Eq. (3.1) $\Sigma^{\text{X}}(\mathbf{k})$ is the exchange, or Fock, part of the self-energy operator and $\Sigma^{\text{C}}(\mathbf{k}; \varepsilon)$ the energy-dependent correlation part. The exchange-correlation potential v^{XC} can be interpreted as the self-energy in the LDA and hence has to be subtracted in Eq. (3.1). Within the GW approximation the self-energy is approximated by the product of the electron Green's function G and the screened interaction W (multiplied by i). In line with common practice, we approximate the electron Green's function by the LDA Green's function and evaluate the screened interaction W in the random-phase approximation (RPA). For the energy dependence (ω dependence) of the screened interaction we use the PPM of Engel and Farid.[25] This PPM yields in the limit $\omega \rightarrow 0$ the correct static expression for the screened interaction and ensures in the limit $\omega \rightarrow \infty$ satisfaction of the Johnson f -sum rule.[51] With these approximations, we find for the correlation part in Eq. (3.1)

$$\langle l, \mathbf{k} | \hbar \Sigma^{\text{C}}(\mathbf{k}; \varepsilon) | l, \mathbf{k} \rangle = \int_{\text{1BZ}} \frac{d^3 q}{(2\pi)^3} \sum_{l' \in \text{EB}} \sum_{m \in \text{PB}} \frac{\left| \sum_{\mathbf{G}} w_{m,\mathbf{q}}^*(\mathbf{G}) \sum_{\mathbf{G}'} d_{l',\mathbf{k}-\mathbf{q}}^{0*}(\mathbf{G}' - \mathbf{G}) d_{l,\mathbf{k}}^0(\mathbf{G}') \right|^2}{\varepsilon - \varepsilon_{l'}(\mathbf{k} - \mathbf{q}) + [\omega_m(\mathbf{q}) - i\eta] \text{sgn}[\mu - \varepsilon_{l'}(\mathbf{k} - \mathbf{q})]}. \quad (3.3)$$

In this expression, EB denotes the electron bands, PB denotes the plasmon bands, η is an infinitesimally small positive energy, and μ is the chemical potential, which in the case of a semiconductor is situated in the energy gap. The $d_{l,\mathbf{k}}^0(\mathbf{G})$ (\mathbf{G} is a reciprocal lattice vector) denotes a plane-wave coefficient of the LDA wave functions. The plasmon coefficients $w_{m,\mathbf{q}}(\mathbf{G})$ and energies $\omega_m(\mathbf{q})$ follow from a generalized eigenvalue problem.[25] A theoretical exposition of this particular PPM is being postponed till Chapter 4. Contrary to other plasmon pole models, which merely serve to give an analytic approximation of the energy dependence of the screened interaction, the plasmon energies of the used PPM can be interpreted physically, at least for the lowest-lying plasmon bands.[25] If nonlocal

pseudopotentials are used, as we have done, it can be shown that the f -sum rule is not exactly obeyed.[24] However, in Ref. [78] it has been concluded that this violation has only a minor effect on QP energies.

In the numerical implementation, wave-vector integrations such as in Eq. (3.3) are replaced by discrete sums. These summations will be performed over the grid

$$\mathbf{q} = (n_1 \mathbf{b}_1 + n_2 \mathbf{b}_2 + n_3 \mathbf{b}_3)/2N_{\text{gr}} \quad (n_i = -N_{\text{gr}} + 1, \dots, N_{\text{gr}}), \quad (3.4)$$

with \mathbf{q} reduced to the 1BZ if necessary. The \mathbf{b}_i are the primitive vectors of the reciprocal lattice. The integrands of the contributions from Σ^X and Σ^C [see Eq. (3.3) for the expectation value of the latter] have a singularity if the wave vector in the Brillouin zone integration vanishes ($\mathbf{q} \rightarrow \mathbf{0}$). This singularity is integrable and is handled analytically in a way similar to that described in Appendix B of Ref. [18]. The only difference is that in the calculation of the contribution of the singular part of the integrand instead of a spherical region an ellipsoidal region is used, which is better adapted to the hexagonal unit cells of the crystals under consideration.

The static dielectric constant ϵ_∞ is defined by $\epsilon_\infty = 1/\lim_{\mathbf{q} \rightarrow \mathbf{0}} \{\epsilon^{-1}(\mathbf{q}; \omega = 0)\}_{\mathbf{G}=\mathbf{0}, \mathbf{G}'=\mathbf{0}}$, where ϵ is the dielectric matrix and is anisotropic in the case of hexagonal symmetry: The transversal (i.e., perpendicular to the c or k_z axis of the hexagonal Brillouin zone) static dielectric constant $\epsilon_{\perp\infty}$ is generally not equal to the longitudinal (i.e., parallel to the c or k_z axis) static dielectric constant $\epsilon_{\parallel\infty}$. For instance, for 6H SiC the experimental values are 6.52 and 6.70, respectively, while for 3C SiC the isotropic value of 6.52 applies.[61] In the simplified GW scheme of WKBC some anisotropic effects of the static dielectric constants were incorporated: The available transversal and longitudinal static dielectric constants of 6H and 3C SiC were used to obtain the ones for 2H and 4H SiC by extrapolation as a function of h . However, it is not evident that the dielectric constants of hexagonal polytypes should vary linearly with h . We use *ab initio* LDA-RPA dielectric matrices as input. In principle, the anisotropy in the limit $\mathbf{q} \rightarrow \mathbf{0}$ in the integrand of Eq. (3.3) could be dealt with. However, because of the fact that the anisotropy is small (for 6H SiC, for instance, it is about 3%) we ignore it altogether and calculate the dielectric matrix and the screened interaction for $\mathbf{q} \rightarrow \mathbf{0}$ in one particular direction. In order to check the validity of this procedure we have investigated the dependence of the calculated QP energies upon this direction and concluded that it is negligible for the materials under consideration.

3.3 Results

In our calculations we used energies and wave functions obtained from well-converged pseudopotential LDA calculations carried through in a plane-wave basis set with a cutoff of 50 Ry, corresponding to the number of plane waves N_{PW} of 1689, 3355, and 5057 for

2H, 4H, and 6H SiC, respectively. To calculate the charge density from the wave functions eight special points in the full irreducible wedge of the 1BZ were used, generated according to Pack and Monkhorst.[67] We used the experimental hexagonal lattice constants[61] $a = 3.0763 \text{ \AA}$ and $c = 5.0480 \text{ \AA}$ for 2H SiC, $a = 3.073 \text{ \AA}$ and $c = 10.053 \text{ \AA}$ for 4H SiC, and $a = 3.0806 \text{ \AA}$ and $c = 15.1173 \text{ \AA}$ for 6H SiC. The distance between the Si and C atom in each Si-C pair was taken equal to the ideal value $3c/4p$ for the polytype p H. The deviations from this ideal value are less than 0.3%.[11, 53] The implemented parametrization of the *ab initio* nonlocal ionic norm-conserving pseudopotentials was that of Bachelet, Greenside, Baraff, and Schlüter.[3] The exchange-correlation potential v^{XC} was represented with the Wigner interpolation formula.[83]

In the calculation of the expectation values and their energy derivatives of the correlation part and the expectation values of the exchange part of the *GW* self-energy [see Eqs. (3.1) — (3.3)] the number of \mathbf{q} points in the wave-vector summations [see Eq. (3.4)] was taken to be 216 ($N_{\text{gr}} = 3$) for 2H and 64 ($N_{\text{gr}} = 2$) for 4H and 6H SiC. In the calculation of the RPA dielectric matrices the same numbers were used, except for the zero-wave-vector limit in the case of 2H SiC for which the number of \mathbf{q} points was taken to be 512 ($N_{\text{gr}} = 4$). In the calculation of the RPA dielectric matrices and the expectation values and their energy derivatives of the correlation part of the self-energy, both N_{PW} and the numbers of electron bands (and plasmon bands in the latter case) taken into account were 287, 563, and 851 for 2H, 4H, and 6H SiC, respectively. In the calculation of the expectation values of the exchange part of the self-energy and the exchange-correlation potential in Eq. (3.1) we took $N_{\text{PW}} = 391, 813, \text{ and } 1211$ for 2H, 4H, and 6H SiC, respectively. With these cutoffs our calculated QP and plasmon energies are converged to within 0.05 eV for 2H SiC and 0.1 eV for 4H and 6H SiC. The $\mathbf{q} \rightarrow \mathbf{0}$ limit of the dielectric matrix and screened interaction was taken along the $\Gamma - A$ axis (see Fig. 3.2). For 2H SiC we have investigated the influence of the anisotropy of the dielectric function on our calculated *GW* quasiparticle energies by taking $\mathbf{q} \rightarrow \mathbf{0}$ along other directions than $\Gamma - A$. The resulting deviations in the *GW* quasiparticle energies were only about 0.02 eV. The effects of anisotropy in 4H and 6H SiC are expected to be even smaller. As a test of our computer code we recalculated the QP and plasmon energies of 3C (cubic) SiC in the hexagonal 6H unit cell and checked our results against those of Ref. [5].

In Fig. 3.1 we have plotted for 2H, 4H, and 6H SiC the two lowest-lying plasmon bands (obtained from the generalized eigenvalue problem of Ref. [25]) as a function of the wave vector at the high symmetry axes $A-L-M-\Gamma-A$ in the 2H, 4H, and 6H 1BZ, respectively. The lowest plasmon energy, which occurs at Γ , is shown to vary barely with the polytype: 22.40, 22.42, and 22.30 eV for 2H, 4H, and 6H SiC, respectively. Only one experimental value of the lowest plasmon energy for both 3C SiC and noncubic polytypes of SiC is known to us, namely, 22.1 eV.[71] The calculated values agree well with this experimental value. It would be interesting to compare our plasmon dispersions with experimental data.

However, as far as we know, measurements of plasmon dispersions for the SiC polytypes have not yet been reported on in the literature.

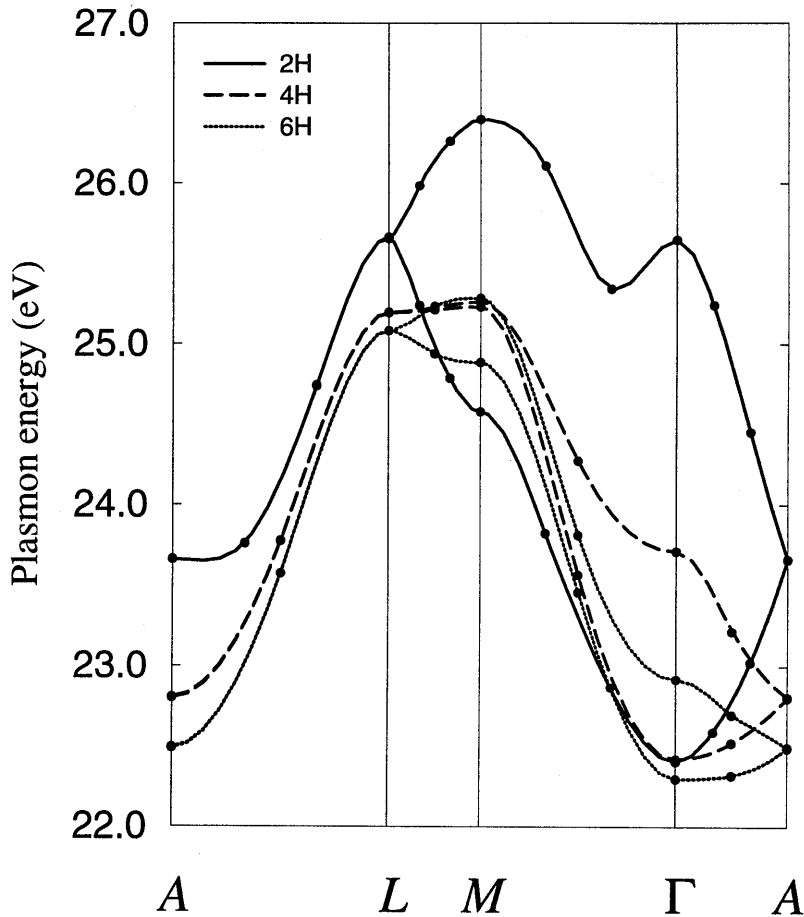


Figure 3.1: Calculated dispersion of the two lowest-lying plasmon bands along some symmetry axes of the hexagonal 1BZ (see Fig. 3.2). The filled circles indicate the actually calculated values. The plotted plasmon energies at Γ were obtained by taking the zero-wave-vector limit along the $\Gamma - A$ axis.

Our LDA and QP energies for 2H, 4H, and 6H SiC for the highest valence band and the lowest conduction band at some high symmetry points in the 1BZ are listed in Table 3.1, together with the corresponding results of WKBC and the experimental data. It is known that in 6H SiC a camel's back structure for the lowest conduction band along the $L-M$ axis exists, but, based on the results of Ref. [60], we assume that taking the lowest conduction band at the M point leads only to a minor error in the calculated GW fundamental gap for 6H SiC. Our calculated GW fundamental band gaps are 3.15, 3.35, and 3.24 eV for 2H, 4H, and 6H SiC, respectively. In comparing these gaps with the absorption gaps of 3.330 eV for 2H SiC[68] and 3.263 and 3.023 eV for 4H and 6H SiC, respectively,[17] we have to account for the exciton binding energies. For 4H and 6H SiC these binding energies are experimentally found to be 0.020 and 0.078 eV[23, 75], respectively, i.e., smaller than the accuracy of our GW calculations. For 2H SiC no value for the exciton binding energy is known to us, but it is hard to believe that the value for this binding energy would be larger than the above-mentioned values. The agreement between our results and the experimental results is very good. The largest difference is found for 2H SiC: 0.18 eV. In Fig. 3.3 we have collected fundamental gap values of the present work, of WKBC, of Rohlfiing *et al.*,[73] and of Backes *et al.*,[5] and the experimental fundamental gaps in a plot of gap versus \hbar . It is clearly seen that the results of the simplified GW calculations of WKBC are in general not as good as those of the more rigorous calculations of the present work and Refs. [5] and [73]. For 6H SiC (one of the polytypes for which WKBC applied the model dielectric function using the available experimental dielectric constants) the result with regard to the fundamental gap is of comparable quality. Concerning the GW values of indirect gaps other than the fundamental gaps, the differences between the results of WKBC and the present work are larger than for the fundamental gaps. It would be interesting to compare the calculated values with experimental values for these other indirect gaps, but we are not aware of such measurements. As far as dielectric constants are concerned, we can only report a reliable value for the longitudinal dielectric constant $\epsilon_{||\infty}$ of 2H SiC: 7.23. This value agrees very well with the theoretical value 7.32 reported in Ref. [16], in which a more systematic study of the dielectric properties of SiC polytypes was performed, and the theoretical value 7.28 reported in Ref. [54].

3.4 Conclusion

Summarizing, *ab initio* plasmon band structures and GW quasiparticle energies have been presented for the 2H, 4H, and 6H polytypes of SiC. Our calculated GW fundamental band gaps are 3.15, 3.35, and 3.24 eV for 2H, 4H, and 6H SiC, respectively; see Table 3.1. Our GW quasiparticle energies improve those of previous simplified GW calculations and are in very good agreement with experimental values. It has been demonstrated that the

GW approximation yields reliable predictions of quasiparticle energies also for this class of materials.

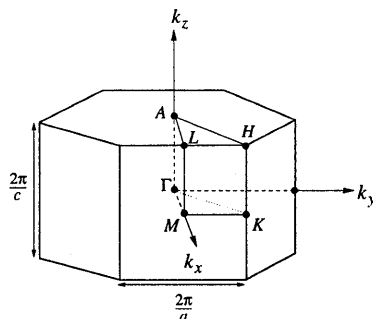


Figure 3.2: Hexagonal Brillouin zone, with a and c the hexagonal lattice constants. Some hexagonal high symmetry points are indicated.

Table 3.1: Quasiparticle energies (in eV) at some high symmetry points of the hexagonal Brillouin zone for 4H and 6H SiC. Results of the present study (also the LDA results are given) as well as those of WKBC are included. The included experimental energies are corrected for exciton binding energies. All energies refer to the valence-band top (Γ_{6v}), which is set at 0 eV.

l, \mathbf{k}	6H				4H			
	LDA	Present	WKBC	Expt.	LDA	Present	WKBC	Expt.
Γ_{6v}	0.00	0.00	0.00	0.00	0.00	0.00	0.00	0.00
Γ_{1c}	5.10	6.57	6.95		5.15	6.44	6.92	
$A_{5,6v}$	-0.08	-0.09	-0.09		-0.20	-0.22	-0.20	
$A_{1,3c}$	5.17	6.64	7.02		5.36	6.65	7.14	
M_{4v}	-1.04	-1.11	-1.40		-1.06	-1.15	-1.23	
M_{1c}	1.82	3.24	3.25	3.10	2.08	3.35	3.56	3.28
$L_{1,2,3,4v}$	-1.23	-1.33	-1.63		-1.50	-1.61	-1.68	
$L_{1,3c}$	1.85	3.29	3.36		2.49	3.80	4.06	

3.4. Conclusion

Table 3.1: continued; for 2H SiC. The included experimental energies are not corrected for exciton binding energies (see the main text).

l, \mathbf{k}	2H			
	LDA	Present	WKBC	Expt.
Γ_{6v}	0.00	0.00	0.00	0.00
Γ_{1c}	4.81	5.83	6.66	
K_{2v}	-3.84	-4.07	-4.12	
K_{2c}	2.01	3.15	3.68	3.33
H_{3v}	-1.67	-1.83	-1.83	
H_{3c}	4.99	6.13	6.86	
$A_{5,6v}$	-0.70	-0.78	-0.75	
$A_{1,3c}$	5.90	6.96	7.81	
M_{4v}	-1.14	-1.25	-1.13	
M_{1c}	2.57	3.67	4.28	
$L_{1,2,3,4v}$	-2.29	-2.48	-2.30	
$L_{1,3c}$	3.16	4.23	4.85	

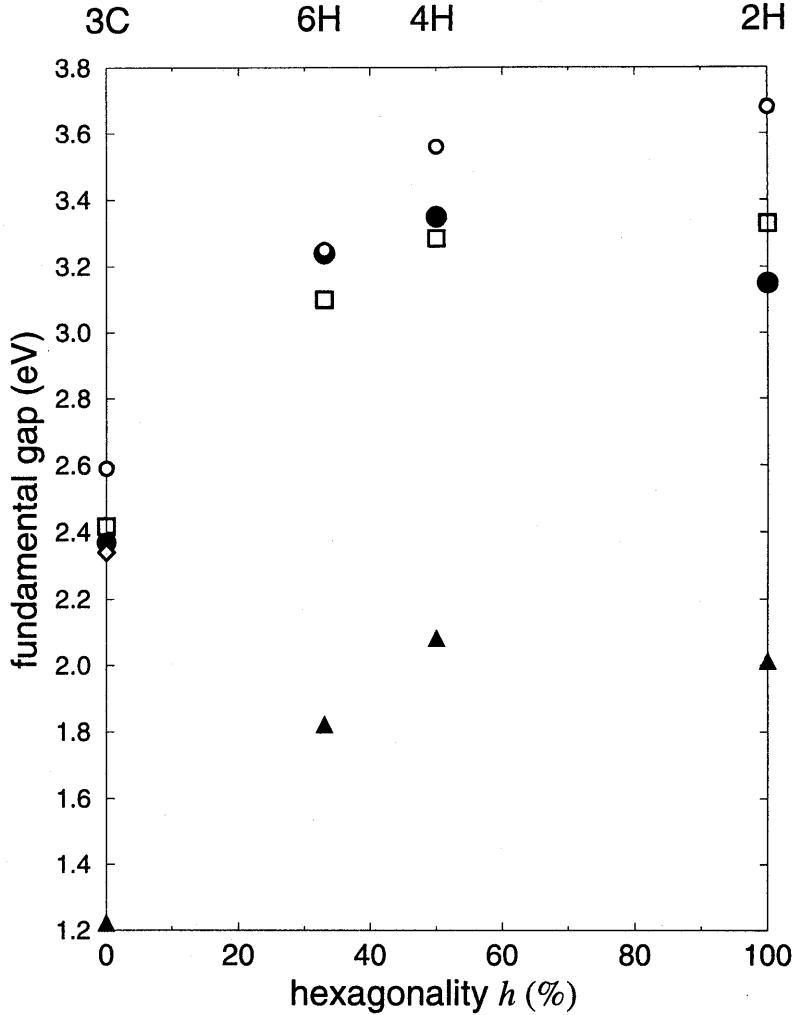


Figure 3.3: Fundamental gap versus percentage hexagonality (h). The results of the present study and the result of Ref. [5] for 3C SiC are indicated by filled circles. The result of Ref. [73] for 3C SiC is indicated by a diamond. Results reported by WKBC are indicated by open circles. The experimental values, corrected for the exciton binding energies (except for 2H SiC; see the main text), are plotted as squares. LDA values are indicated by triangles, in order to show the effect of GW.

Chapter 4:

First-order corrections to RPA-GW calculations in silicon and diamond.

Published in *R.T.M. Ummels, P.A. Bobbert, and W. van Haeringen, Phys. Rev. B 57, 11 962 (1998).[78]*

Abstract

We report on *ab initio* calculations of the first-order corrections in the screened interaction W to the random-phase approximation polarizability and to the GW self-energy, using a noninteracting Green's function, for silicon and diamond. It is found that the first-order vertex and self-consistency corrections to the polarizability largely compensate each other. This does not hold, however, for the first-order corrections to the GW gap. For silicon the compensation between the first-order vertex and self-consistency correction contributions to the gap is only about 35%, while for diamond it is even absent. The resulting gap values are significantly and systematically too large, the direct gaps for silicon and diamond being 0.4 eV and 0.7 eV larger than their GW values, respectively. The success of GW in predicting electronic properties of, e.g., silicon and diamond can therefore apparently not be understood in terms of "small" corrections to GW to first order in W using a noninteracting Green's function.

4.1 Introduction

One of the most successful methods of describing exchange-correlation effects in *ab initio* calculations is the random-phase approximation (RPA) GW approach, where the (irreducible) polarizability P is calculated in the RPA and the self-energy Σ is calculated to first order in the dynamically screened interaction W . [44, 45] It is remarkable in this connection that non-self-consistent RPA- GW calculations lead to quasiparticle (QP) band gaps that are in excellent agreement with experiment in the case of a large group of semiconductors if the starting point is chosen to be the density-functional theory (DFT) in the

local-density approximation (LDA). Henceforth we will call this non-self-consistent RPA-GW approach “standard GW”. The inherent assumption that higher-order corrections can be neglected is, however, far from obvious.

The inclusion of vertex (V) and so-called self-consistency (SC) corrections to Σ and P has been studied by a number of researchers, mainly for the homogeneous electron gas. Hubbard[47] introduced the corrections to the RPA by means of a local-field factor (not to be confused with the so-called local-field effects to be introduced later on). In the electron gas case much effort has gone into obtaining expressions for local-field factors in the dielectric function; see, for instance, Refs. [14] and [45]. DuBois[22], whose work can be considered as an extension to the work of Gell-Mann and Brueckner[32, 33], stresses the importance of taking into account all polarizability diagrams of the same order in the Wigner-Seitz radius r_s . He noticed the significant cancellation between V and SC corrections in the high density limit. Geldart and Taylor[31] found a similar compensation for the static polarizability. They attempted to construct a local-field factor that includes SC corrections. Mahan and Sernelius[65], using the local-field factor approach, concluded that the effects of V corrections to the bandwidth of the homogeneous electron gas nearly cancel when added to both the self-energy and the polarizability, as was already predicted by Rice[72].

In a recent paper of Shirley[76] a self-consistent GW (SCGW) calculation is reported on for the homogeneous electron gas, in which, however, a fixed screened interaction is employed. The resulting bandwidth is found to be appreciably larger than the (assumed) more correct standard GW value. A similar result is obtained by von Barth and Holm[9], who performed a full SCGW calculation by including the screened interaction in the self-consistency procedure. Shirley[76] furthermore reports on a nearly self-consistent calculation to second order in the screened interaction W , i.e., by incorporating, apart from the GW diagram, also the first-order vertex correction diagram to GW. The employed Green’s function G in this calculation is the one obtained from his SCGW calculation, however. The resulting bandwidth in this latter calculation is found to be very close to the standard GW value. This is indicative for a strong compensation between V and SC corrections, fully in line with arguments put forward in Refs. [10] and [80].

Calculations for inhomogeneous systems are much more difficult to perform, which explains that the situation concerning corrections to standard GW is much less settled for such systems. In Ref. [36] a full SCGW calculation was presented for the relatively simple case of a quasi-one-dimensional semiconducting wire. It resulted in a value for the band gap that is large compared to the standard GW band-gap value. The obtained result appears to be completely at variance with the much smaller band gap obtained in the quantum Monte Carlo (QMC) calculation for this system presented in Refs. [56] and [57]. The QMC value should for reasons of principle lie close to the “exact” band-gap value; it appears to be close to the standard GW value. The apparent difference between the SCGW and

QMC results strongly points to the need of including vertex corrections in the former type of calculation, like the SCGW result for the electron gas in Refs. [9] and [76]. Indeed, in Ref. [37] it was found that the band gap is much closer to the standard GW band gap and the QMC band gap, if all first-order corrections to *both* the RPA polarizability and the GW self-energy are systematically included.

As far as calculations on real semiconductors are concerned, we note that Hanke and Sham [42] included V corrections to the RPA polarizability for a covalent crystal (diamond), using the bare Coulomb interaction instead of the dynamically screened interaction. Concerning the importance of vertex corrections to the self-energy, Daling and van Haeringen [18], Daling *et al.*[19], and Bobbert and van Haeringen [13] conclude that the effect of the first-order vertex correction to the standard GW self-energy on the direct band gap at the Γ point of silicon is relatively small. The former results[18, 19] were obtained by using the bare Coulomb interaction, the latter [13] by using the dynamically screened interaction. Del Sole, Reining, and Godby[20] have arrived at a similar conclusion for silicon on the basis of a so-called $GW\Gamma$ calculation, which incorporates in an approximate way vertex corrections to the self-energy as well as to the polarizability, by means of the functional derivative of the exchange-correlation potential in DFT with respect to the density. Bechstedt *et al.*[11] have shown that dynamical effects due to vertex corrections and self-consistency corrections to the strength of the optical absorption (and correspondingly P) largely cancel for silicon and diamond.

The present work can be seen as an extension of Ref. [37] and also of Ref. [13]. The aim is to contribute further to the understanding of the success of standard GW . In considering possible improvements to standard GW , Hedin[44] argues that one should preferably take Σ to n th order in W if P is taken to order $n-1$ in W , provided both Σ and P are taken self-consistently. In view of the complexity of dealing with self-consistency and higher-order corrections, we will restrict ourselves to the investigation of the effect of including the first-order corrections in W to standard GW as well as to the RPA P . Not a self-consistent Green's function, but the LDA Green's function will be employed in this investigation. Two aspects concerning the screened interaction W are essential in an accurate evaluation of QP energies for semiconductors: first, its energy dependence, and, second, the off-diagonal matrix elements of P in the employed plane-wave basis set, giving rise to the so-called local-field effects (LFE). Both dynamical screening and LFE will be included in our calculations. The energy dependence of the dynamically screened interaction will be modeled by means of the plasmon pole model (PPM) of Engel and Farid [25]. We will consider three kinds of calculations: (i) calculation of the first-order $V+SC$ correction to the RPA polarizability using the RPA screening, (ii) calculation of the first-order $V+SC$ correction to the GW self-energy using the RPA screening, and (iii) calculation of the GW self-energy and its first-order corrections using the corrected screening from (i). The calculation of these corrections to standard GW is done for both silicon and diamond, with

emphasis on the energy levels around the band gap.

The paper is organized as follows. In Section 4.2 we will discuss the diagrams that have to be taken into account for P and Σ and we will give a short description of some calculational details. In Section 4.3 we will give the results. In Section 4.3.1 we will focus on the polarizability. In Section 4.3.2 results for the self-energy are given, concentrating on energy levels around the band gap. A few checks are carried through in Section 4.4. Section 4.5 contains a further discussion concerning the SC self-energy correction. In Section 4.6 we report on a remarkable cancellation between a particular group of second-order corrections to the LDA energy gap. Section 4.7 is devoted to the discussion of our results.

4.2 Theory

The RPA polarizability diagram as well as its first-order correction Feynman diagrams are depicted in Fig. 4.1. The GW self-energy diagram as well as its first-order correction Feynman diagrams are depicted in Fig. 4.2. Diagrams SC1 — SC4 are the first-order self-consistency diagrams since they have self-energy insertions in the Green's functions, taking into account self-consistency effects to first order. The cross in diagrams SC2 and SC4 denotes minus the LDA exchange-correlation potential, $-v^{\text{XC}}$. These latter diagrams should be included when the LDA is the starting point because v^{XC} can be considered as the self-energy in the LDA, which should be canceled out. Diagrams SC3 and SC4 of Fig. 4.2 are self-energy corrections due to the first-order corrections to the valence charge density. We will henceforth call these latter diagrams SC Hartree diagrams. Diagram V is the first-order vertex correction diagram.

In the evaluation of the corrections to the wave-vector-dependent and energy-dependent polarizability $P_{\mathbf{G},\mathbf{G}'}(\mathbf{k};\omega)$ and self-energy $\Sigma_{\mathbf{G},\mathbf{G}'}(\mathbf{k};\omega)$ in a plane-wave basis (\mathbf{G} and \mathbf{G}' are reciprocal lattice vectors, \mathbf{k} is the wave vector, and ω is the energy) one wave-vector integration can be reduced to an integration over the \mathbf{k} -dependent irreducible wedge $\mathcal{I}_{\mathbf{k}}$. The second wave-vector integration, if present, cannot be reduced and has to be performed over the whole first Brillouin zone (1BZ). Furthermore, in our calculations, wave-vector integrations have been replaced by a discrete sum over the wave vectors of the grid

$$\mathbf{q} = (n_1\mathbf{b}_1 + n_2\mathbf{b}_2 + n_3\mathbf{b}_3)/2N_{\text{gr}} \quad (n_i = -N_{\text{gr}} + 1, \dots, N_{\text{gr}}), \quad (4.1)$$

with \mathbf{q} reduced to the 1BZ if necessary, where \mathbf{b}_i are the primitive vectors of the reciprocal lattice. A specific \mathbf{q} -point set will be identified by giving the number N_{gr} . The integrand pertaining to a particular correction may have a singularity if the wave vector in an interaction line goes to zero. Such singularities are all integrable and are handled analytically in a way described in Appendix B of Ref. [18].

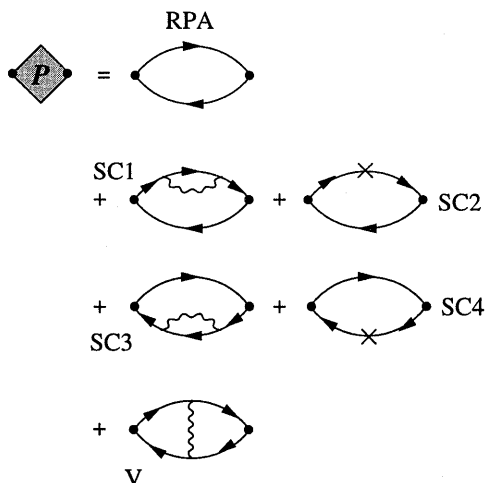


Figure 4.1: RPA polarizability plus the first-order corrections to it. SC1 — SC4 denote the first-order self-consistency corrections. V denotes the first-order vertex correction. The solid directed line denotes the LDA Green's function. The cross denotes $-v^{XC}$. The wiggly line denotes the RPA dynamically screened interaction.

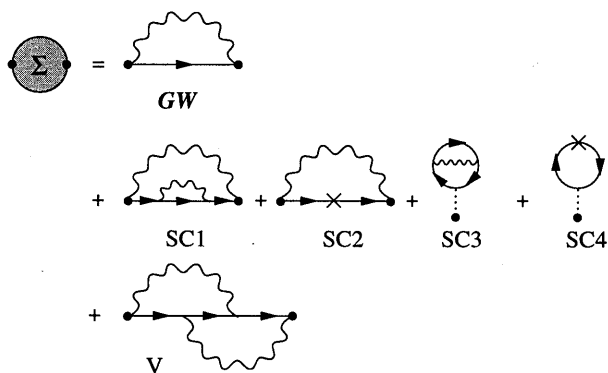


Figure 4.2: GW self-energy plus the first-order corrections Σ^{V+SC} . The dotted line denotes the bare Coulomb interaction. The wiggly line now denotes the dynamically screened interaction obtained with either the RPA or the RPA+V+SC polarizability; see Fig. 4.1.

The energy-dependent screened interaction $W_{\mathbf{G},\mathbf{G}'}(\mathbf{q};\omega)$ can be written as (shorthand notation)

$$W = v + v\chi v \equiv v + W^{\text{scr}}, \quad (4.2)$$

where χ is the full polarizability matrix and v is the bare Coulomb interaction, $v_{\mathbf{G},\mathbf{G}'}(\mathbf{q}) = e^2\delta_{\mathbf{G},\mathbf{G}'}/(\epsilon_0|\mathbf{q} + \mathbf{G}|^2)$. We use SI units: e is the electron charge and ϵ_0 is the vacuum permittivity. The full polarizability χ is related to the (irreducible) polarizability P by

$$\chi = P(I - vP)^{-1}, \quad (4.3)$$

where I denotes the unit matrix. We will use a representation for the screening part of W , W^{scr} , that is analogous to the Lehmann representation for the noninteracting (LDA) Green's function G^0 :

$$G_{\mathbf{G},\mathbf{G}'}^0(\mathbf{k};\omega) = \hbar \sum_l \frac{d_{l,\mathbf{k}}^0(\mathbf{G})d_{l,\mathbf{k}}^{0*}(\mathbf{G}')}{\omega - \varepsilon_l(\mathbf{k}) + i\eta \operatorname{sgn}[\varepsilon_l(\mathbf{k}) - \mu]}, \quad (4.4)$$

where the infinitesimally small positive energy η ensures the correct causal behaviour, μ is the chemical potential, which in the case of a semiconductor is situated in the energy gap, and ε_l and d_l^0 are the energies and plane-wave coefficients, respectively, of the starting point wave functions, for instance, obtained within the LDA. Engel and Farid[25] developed a plasmon-pole model (PPM) that provides an analytical approximation for the energy dependence of the dynamically screened interaction W^{scr} , such that energy integrals occurring in expressions for the self-energy and the polarizability can be carried out analytically. The wave-vector-dependent plasmon energies ω_m in this PPM are obtained from the generalized eigenvalue problem[25] (in matrix notation)

$$\underline{\chi}(\mathbf{q};\omega = 0) \mathbf{x}_{m,\mathbf{q}} = -\frac{1}{\omega_m^2(\mathbf{q})} \underline{M}(\mathbf{q}) \mathbf{x}_{m,\mathbf{q}}. \quad (4.5)$$

If the eigenvectors $\mathbf{x}_{m,\mathbf{q}}$ of Eq. (4.5), with components $x_{m,\mathbf{q}}(\mathbf{G})$, are normalized according to $\mathbf{x}_{m,\mathbf{q}}^\dagger \underline{M}(\mathbf{q}) \mathbf{x}_{n,\mathbf{q}} = \delta_{m,n}$ and satisfy the completeness relation $\sum_m \mathbf{x}_{m,\mathbf{q}} \mathbf{x}_{m,\mathbf{q}}^\dagger = \underline{M}^{-1}(\mathbf{q})$, then the following plasmon pole description for W^{scr} can be derived[25]:

$$W_{\mathbf{G},\mathbf{G}'}^{\text{scr}}(\mathbf{q};\omega) = \sum_m w_{m,\mathbf{q}}(\mathbf{G}) w_{m,\mathbf{q}}^*(\mathbf{G}') \left\{ \frac{1}{\omega - \omega_m(\mathbf{q}) + i\eta} - \frac{1}{\omega + \omega_m(\mathbf{q}) - i\eta} \right\}, \quad (4.6)$$

where $w_{m,\mathbf{q}} = \underline{v}(\mathbf{q}) \underline{M}(\mathbf{q}) \mathbf{x}_{m,\mathbf{q}} / \sqrt{2\omega_m(\mathbf{q})}$. Within this particular PPM χ is approximated by $\tilde{\chi}$,

$$\tilde{\chi}(\mathbf{q};\omega) = \left\{ \omega^2 \underline{M}^{-1}(\mathbf{q}) + \underline{\chi}^{-1}(\mathbf{q};\omega = 0) \right\}^{-1}. \quad (4.7)$$

For $\omega = 0$ the model full polarizability $\tilde{\chi}$ obviously coincides with χ . Further, the correct $\omega \rightarrow \infty$ limit can be obtained by inserting a properly chosen matrix M . In connection

with the application of plasmon pole models it is desirable [49, 64] to satisfy the Johnson f -sum rule[51]. When using a local one-electron Hamiltonian, this leads to

$$M_{\mathbf{G},\mathbf{G}'}(\mathbf{q}) = \frac{\hbar^2}{m}(\mathbf{q} + \mathbf{G}) \cdot (\mathbf{q} + \mathbf{G}') \rho_{\mathbf{G}-\mathbf{G}'}, \quad (4.8)$$

where $\rho_{\mathbf{G}}$ are Fourier components of the valence charge density. The Johnson f -sum rule and, accordingly, Eq. (4.8) are not exact, however, if the Hamiltonian contains a nonlocal ion pseudopotential. This is pointed out in Refs. [24] and [49]. The resulting violation of the Johnson f -sum rule may very well be of importance in the evaluation of corrections to the GW self-energy.[27] The correct matrix M can easily be obtained by combining Eqs. (4.3) and (4.7) for $\omega \rightarrow \infty$:

$$M_{\mathbf{G},\mathbf{G}'}(\mathbf{q}) = \lim_{\omega \rightarrow \infty} \omega^2 P_{\mathbf{G},\mathbf{G}'}(\mathbf{q}; \omega) \quad (4.9)$$

and extracting the $\omega \rightarrow \infty$ behaviour of the polarizability P . In this limit the leading term of P is proportional to $1/\omega^2$. In Section 4.3.2 we will investigate the effects of the violation of the Johnson f -sum rule. The standard GW band gap of semiconductors calculated with the PPM based on Eq. (4.8) is in excellent agreement with experiment for silicon and diamond [see Section 4.3.2], 3C SiC [5, 73], and 2H, 4H, and 6H SiC [see Chapter 3 of this thesis].

When splitting the screened interaction W into its static part v and dynamic part W^{scr} and by taking into account each possible time order of the internal and external points of a diagram, specific subdiagrams of Σ and P can be identified. For the polarizability diagram V of Fig. 4.1 we get a total of 30 subdiagrams. This can be seen as follows: There are 3! possible time orders if the bare Coulomb interaction v is taken and 4! possible time orders if W^{scr} is taken. For diagrams SC1 plus SC3 of Fig. 4.1 there are $2 \times 3!$ subdiagrams, while diagrams SC2 plus SC4 lead to $2 \times 3!$ subdiagrams. For the self-energy diagram V of Fig. 4.2 there are 38 subdiagrams (for more details see Ref. [13]). For diagram SC1 of Fig. 4.2 there are also 38 subdiagrams, for diagram SC2 $2!+3!$ subdiagrams, and for diagrams SC3 and SC4 $2!+3!$ and $2!$ subdiagrams, respectively.

In Appendix A the contribution pertaining to one specific subdiagram of the first-order vertex correction polarizability diagram, diagram V in Fig. 4.1, is given as an example. We want to emphasize that the head element (HE) ($\mathbf{G} = \mathbf{0}$ and $\mathbf{G}' = \mathbf{0}$) and the wing elements (WE) ($\mathbf{G} = \mathbf{0}$ or $\mathbf{G}' = \mathbf{0}$) of the polarizability matrix $P_{\mathbf{G},\mathbf{G}'}(\mathbf{k}; \omega)$ have to be treated in a special way for $\mathbf{k} \rightarrow \mathbf{0}$ in the case of semiconductors. In the case of the RPA polarizability the HE has a $|\mathbf{k}|^2$ proportionality and the WE have a linear \mathbf{k} proportionality for $\mathbf{k} \rightarrow \mathbf{0}$, leading to the correct screening behaviour of a semiconductor. Individually, none of the diagrams V and SC in Fig. 4.1 has the property that the HE is proportional to $|\mathbf{k}|^2$ for $\mathbf{k} \rightarrow \mathbf{0}$. Only the sum of these diagrams fulfills this property. Kohn[58] has proved this for the case that the interaction line represents the bare Coulomb interaction, but it can

also rather easily be proved for the screened interaction W . We have chosen to tackle the evaluation of the V+SC polarizability correction in the $\mathbf{k} \rightarrow \mathbf{0}$ limit numerically in the following way: The HE of the V+SC correction is evaluated for three small \mathbf{k} vectors and then fitted according to

$$\Delta P_{\mathbf{0},\mathbf{0}}(\mathbf{k} \rightarrow \mathbf{0}) := p_0 + p_1|\mathbf{k}| + p_2|\mathbf{k}|^2. \quad (4.10)$$

The WE of the V+SC correction are evaluated for four small \mathbf{k} vectors and then fitted according to

$$\Delta P_{\mathbf{0},\mathbf{G} \neq \mathbf{0}}(\mathbf{k} \rightarrow \mathbf{0}) := p_0 + p^x k_x + p^y k_y + p^z k_z. \quad (4.11)$$

Here p_0 , p_1 , p_2 , p^x , p^y , and p^z are fitting parameters. In Eq. (4.11) the fitting parameters are \mathbf{G} dependent.

Having obtained the polarizability P , the calculation of the dielectric matrix ϵ can easily be accomplished by evaluating $\epsilon = I - vP$. In the calculation of the dielectric matrix for $\mathbf{k} \rightarrow \mathbf{0}$ the $1/|\mathbf{k}|^2$ singularity of the HE of the bare Coulomb interaction is canceled by the $|\mathbf{k}|^2$ behaviour of the HE of the polarizability. Likewise the singularity of the WE of the bare Coulomb interaction is canceled. The macroscopic response to an applied field is determined by ϵ^{-1} rather than ϵ . In accordance with Ref. [50], we define a macroscopic dielectric function (MDF) by

$$\epsilon_M(\mathbf{q} + \mathbf{G}) := \frac{1}{\{\epsilon^{-1}(\mathbf{q}; \omega = 0)\}_{\mathbf{G},\mathbf{G}}}. \quad (4.12)$$

The effects of the off-diagonal matrix elements of the dielectric function are often referred to as the local-field effects (LFE). The macroscopic or static dielectric constant ϵ_∞ is given by $\epsilon_\infty = \lim_{\mathbf{q} \rightarrow 0} \epsilon_M(\mathbf{q})$. For cubic crystals the static dielectric constant is independent of the direction in which the wave vector goes to zero. In the LDA-RPA the static dielectric constant is generally overestimated in the case of semiconductors; see, for instance, Refs. [24] and [50].

Since the GW wave functions in silicon and diamond are practically undistinguishable from the LDA wave functions, it is sufficient to calculate diagonal matrix elements of the GW self-energy in the LDA basis when evaluating QP energies.[35, 49] In order to account for the fact that the expectation values should be evaluated at the QP energies, the self-energy is expanded to first order in the difference between the QP and the LDA energies to obtain the desired QP energies $E_l^{\text{QP}}(\mathbf{k})$, leading to

$$E_l^{\text{QP}}(\mathbf{k}) = \varepsilon_l(\mathbf{k}) + Z_{l,\mathbf{k}} \hbar \langle l, \mathbf{k} | \Sigma(\mathbf{k}; \varepsilon_l(\mathbf{k})) | l, \mathbf{k} \rangle, \quad (4.13)$$

where $Z_{l,\mathbf{k}}$ is the so-called wave-function renormalization factor, given by

$$Z_{l,\mathbf{k}} = \left(1 - \hbar \langle l, \mathbf{k} | \frac{\partial \Sigma(\mathbf{k}; \omega)}{\partial \omega} \Big|_{\omega = \varepsilon_l(\mathbf{k})} | l, \mathbf{k} \rangle \right)^{-1}, \quad (4.14)$$

and $|l, \mathbf{k}\rangle$ indicates a LDA state with band index l and wave vector \mathbf{k} . In the procedure of obtaining QP energies we will therefore evaluate both the expectation values $\hbar\langle l, \mathbf{k} | \Sigma(\mathbf{k}; \varepsilon_l(\mathbf{k})) | l, \mathbf{k}\rangle$ and their derivatives δ ,

$$\delta_l(\mathbf{k}) \equiv \hbar\langle l, \mathbf{k} | \left. \frac{\partial \Sigma(\mathbf{k}; \omega)}{\partial \omega} \right|_{\omega = \varepsilon_l(\mathbf{k})} | l, \mathbf{k}\rangle. \quad (4.15)$$

Here $\hbar\Sigma$ will equal either $-v^{\text{XC}} + \hbar\Sigma^{\text{GW}}$ or $-v^{\text{XC}} + \hbar\Sigma^{\text{GW}} + \hbar\Sigma^{\text{V+SC}}$, depending on whether we are calculating GW or GW+V+SC (GW plus its first order in W corrections) quasi-particle energies. We will refer to the above method of calculating QP energies as the “expectation value method”. This method turns out to work well for the GW self-energy and in Section 4.3.2 we will check its validity for the V+SC self-energy correction. To this end, the result obtained with the expectation value method will be compared with the result of an exact diagonalization of the nonlocal, energy-dependent Hamiltonian $H_0 + \hbar\Sigma$.

4.3 Results

In the calculations to be reported on below we used energies and wave functions obtained from a well-converged self-consistent LDA calculation carried through in a plane-wave basis set with a cutoff of 17 and 45 Ry for silicon and diamond, respectively. We used the experimental lattice constants[61] $a = 5.43 \text{ \AA}$ and $a = 3.57 \text{ \AA}$ for silicon and diamond, respectively. The implemented parametrization of the *ab initio* nonlocal ionic norm-conserving pseudopotentials is that of Bachelet, Greenside, Baraff, and Schlüter.[3] The exchange-correlation potential v^{XC} is represented with the Wigner interpolation formula.[83] Unless indicated otherwise, the matrix M of Eq. (4.8) is used to obtain W^{scr} .

Three cutoffs are to be distinguished in the calculations of P and Σ : (i) the number of plane waves taken into account in reciprocal lattice vector summations and used for the size of dielectric (and polarizability) matrices N_{PW} , (ii) the number of electron and plasmon bands taken into account in band summations N_b , and (iii) the fineness of the \mathbf{k} -space grid in the Brillouin zone integrations N_{gr} ; see Section 4.2. For the polarizability as well as the self-energy $N_{\text{PW}} = 137$ is taken for silicon and $N_{\text{PW}} = 229$ is taken for diamond. For the RPA polarizability and the GW self-energy, N_b is taken equal to N_{PW} . For the V+SC polarizability correction this number is $N_b = 29$ for silicon and $N_b = 30$ for diamond (the choice of N_b is restricted to specific values due to the degeneracy of bands, which has to be properly dealt with for $\mathbf{k} \rightarrow \mathbf{0}$). The contributions to the expectation values and their energy derivatives δ (evaluated at the LDA energies; see Section 4.2) of the V+SC self-energy correction diagrams have been obtained by using $N_b = 65$. In the calculation of the RPA polarizability for $\mathbf{k} \rightarrow \mathbf{0}$, $N_{\text{gr}} = 6$ for silicon and $N_{\text{gr}} = 4$ for diamond is used.

For other \mathbf{k} vectors we use $N_{\text{gr}} = 3$ for silicon and $N_{\text{gr}} = 2$ for diamond. Also, the V+SC polarizability correction is calculated with these latter N_{gr} values for all \mathbf{k} vectors. This holds also for the GW self-energy and its corrections. An exception to this choice of N_{gr} is made for the V+SC correction in the case of the X and L points of silicon, where we assumed that $N_{\text{gr}} = 2$ would also be sufficient, as it turned out to be sufficient to use $N_{\text{gr}} = 2$ for the V+SC correction in the case of the Γ point of silicon.

Convergence tests have been performed in order to assess the accuracy of calculated QP gaps: For silicon, the V+SC correction to the RPA polarizability has also been calculated by taking $N_{\text{PW}} = 89$ and $N_b = 50$ ($N_{\text{gr}} = 2$). This led to the conclusion that the matrix elements of the polarizability corrections were nicely converged, while the effect on the band gap was minor. The V+SC correction to the GW self-energy for the Γ point of silicon and diamond, using RPA screening, has also been calculated by taking $N_{\text{gr}} = 2$, together with taking a smaller N_{PW} ($N_{\text{PW}} = 89$ and 169 for silicon and diamond, respectively) or with more plasmon and electron bands ($N_b = 89$). For diamond the calculations with RPA screening were also done for $N_{\text{gr}} = 3$. We claim on the basis of the above-mentioned convergence tests that the accuracy of reported QP gaps is 0.05 eV for silicon and 0.1 eV for diamond. In Tables 4.2 and 4.3 we nevertheless express numbers with three decimal places in order to clarify possible cancellation effects.

4.3.1 First-order corrections to the RPA polarizability

Unless stated otherwise (see Section 4.3.2), we use the PPM described in Section 4.2 based on the matrix M of Eq. (4.8) in which case we can restrict ourselves to the calculation of the static polarizability $P_{\mathbf{G},\mathbf{G}'}(\mathbf{k}; \omega = 0)$.

In Fig. 4.3 the RPA, V, and SC contributions to the diagonal elements of the static polarizability are shown as a function of the absolute wave vector $|\mathbf{k} + \mathbf{G}|$. The scattering of the points in this figure reflects the anisotropy. One observes that the V and SC contributions compensate each other to a very large degree. The V contribution has the same sign as the RPA polarizability, while the SC contribution has the opposite sign. In absolute value both corrections are roughly 75% of the RPA. The compensation between V and SC is such that the diagonal matrix elements of the RPA+V+SC polarizability are in absolute value a little bit larger than the RPA ones (about 15%). Also in Ref. [37] this compensation was seen for the quasi-one-dimensional semiconducting wire, although the compensation was less complete there. In Fig. 4.3 the constant terms for $\mathbf{k} \rightarrow \mathbf{0}$ ($\mathbf{G} = \mathbf{0}$) for the V and the SC contributions are also given. They are clearly seen to cancel. This is in agreement with Ref. [58], where it has been shown that, for semiconducting crystals, $P_{\mathbf{0},\mathbf{0}}(\mathbf{k}; \omega)$ is proportional to $|\mathbf{k}|^2$ for small $|\mathbf{k}|$.

In Fig. 4 we have plotted the difference between the RPA+V+SC and the RPA MDF as a function of the absolute wave vector $|\mathbf{k} + \mathbf{G}|$. For the definition of the MDF, see

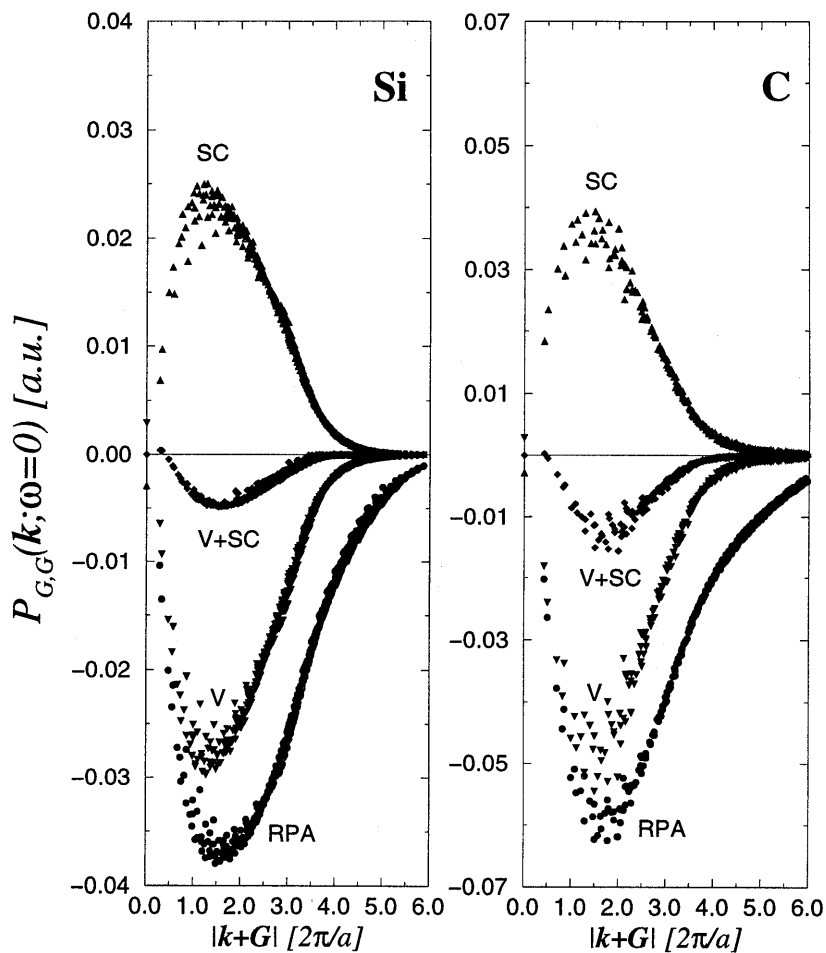
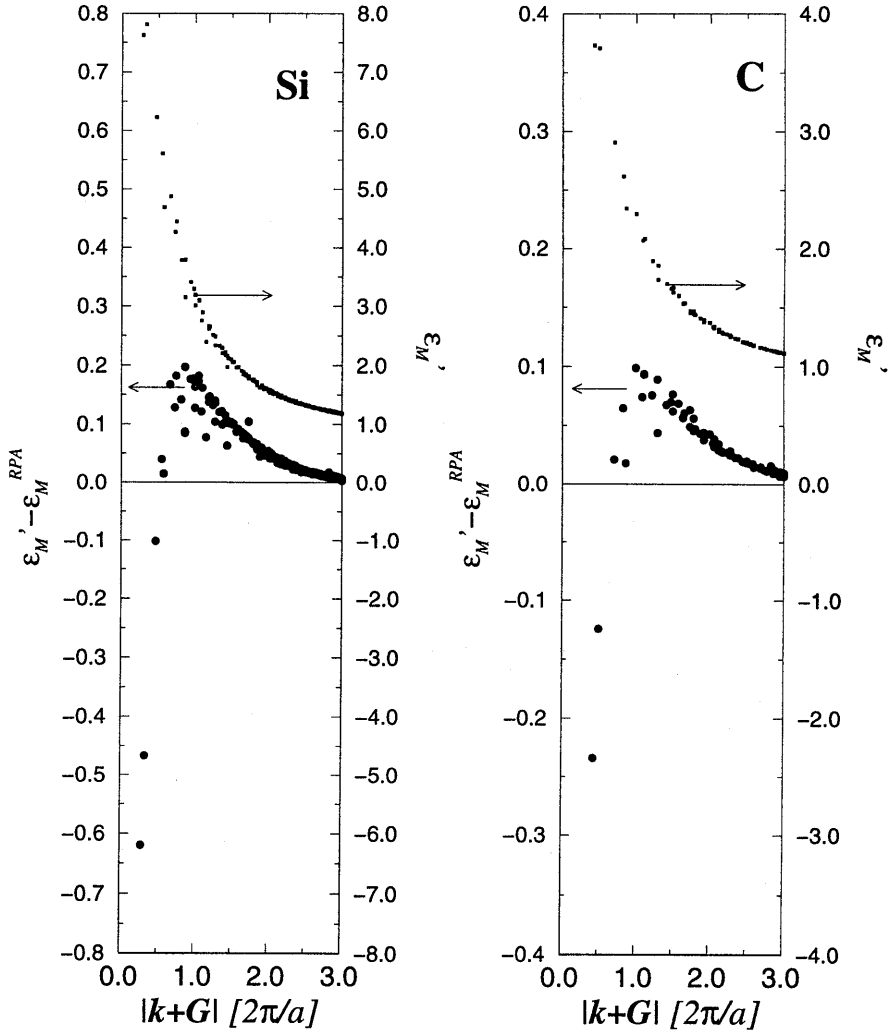


Figure 4.3: Compensation between V and SC corrections to the diagonal elements of the static polarizability (in Rydberg atomic units) for silicon and diamond. The constant contributions to the HE of the polarizability matrix for $\mathbf{k} \rightarrow \mathbf{0}$ are also given (the $|\mathbf{k} + \mathbf{G}| = 0$ axis).

Figure 4.4: RPA+V+SC macroscopic dielectric function (MDF) as well as the difference between the RPA+V+SC and the RPA MDF for silicon and diamond. The definition of the MDF is given in Eq. (4.12). By ϵ'_M we mean $\epsilon_M^{\text{RPA+V+SC}}$. The value of $\epsilon'_M - \epsilon_M^{\text{RPA}}$ for $|\mathbf{k} + \mathbf{G}| \rightarrow 0$ is -2.4 for silicon and -0.3 for diamond (see main text).



Eq. (4.12). The correction is negative for small $|\mathbf{k} + \mathbf{G}|$ and positive for larger $|\mathbf{k} + \mathbf{G}|$. Our obtained RPA+V+SC static dielectric constant is $\epsilon_\infty = 10.4$ and 5.3 in our best calculation for silicon and diamond, respectively, to be compared with our RPA values of 12.8 and 5.6 and with experimental values 11.4 [28, 63], 11.7 [55] and 5.5 [55], 5.7 [70]. So by incorporating the V+SC polarizability correction, we find a decrease in the static dielectric constant. This is contrary to previous results in cases in which the local-density-functional formalism is used to go beyond RPA, which generally show an increase in the static dielectric constant; see, for instance, Ref. [50]. In Refs. [15] and [50], the MDF in the local-density-functional formalism was compared to the RPA MDF. In Ref. [50] the QMC exchange-correlation potential as parametrized by Perdew and Zunger[69] was used, while the Slater exchange-correlation potential was used in Ref. [15]. Comparing our results for the MDF for silicon with Refs. [15] and [50], we observe that our V+SC correction to the RPA MDF is about five times smaller.

To conclude the discussion of the polarizability we can say that the sum of the first-order vertex and self-consistency corrections to the static polarizability is relatively small, with the LDA as the starting point. Our results confirm our previous results for the quasi-one-dimensional semiconducting wire and results of other authors that the V and SC corrections to the polarizability compensate each other to a large degree. Our results can be considered to be complementary to the work of Bechstedt *et al.*[11], who observed such a compensation at finite frequencies, also for silicon and diamond, but without taking LFE into account.

4.3.2 First-order corrections to the GW self-energy

Our standard GW results, obtained by applying the expectation value method, are shown in Table 4.1. The gap values for the Γ , X , and L points of silicon of 3.31 , 4.20 , and 3.38 eV are observed to compare reasonably with the values 3.35 , 4.43 , and 3.54 eV of Ref. [49] and excellently with the experimental values[2, 61] of 3.40 , 4.25 , and 3.45 eV. The result for the Γ point of diamond of 7.63 eV compares well with the 7.5 eV value reported in Ref. [49] and the 7.63 eV value of Ref. [73] and reasonably with the experimental value[61] of 7.3 eV. We remark in this connection that if we take $N_{\text{gr}} = 3$ instead of $N_{\text{gr}} = 2$, our standard GW result for diamond changes from 7.63 eV to 7.54 eV. In Table 4.1 also the GW gap values with RPA+V+SC screening are given. It is observed that the differences between the standard GW and GW /RPA+V+SC gap values are relatively minor, as could be expected from the closeness of the RPA and RPA+V+SC screening (see Section 4.3.1).

We now turn to the first-order vertex and self-consistency self-energy corrections to the GW self-energy. We recall Hedin's argument[44] to take Σ to n th order in W when P is taken to order $n - 1$ in W and our restriction of using the LDA Green's function. In following this line of reasoning when calculating the GW +V+SC self-energy, the resulting

gap values obtained with RPA+V+SC screening should obviously be preferred. From Table 4.1 it is observed that both the $GW+V+SC/RPA$ and the $GW+V+SC/RPA+V+SC$ gap values, obtained by applying the expectation value method, differ considerably from the standard GW values. The differences with the standard GW values appear to be largest if we take the screening to be RPA+V+SC. For this type of screening the differences amount to 0.36, 0.44, and 0.39 eV for the Γ , X , and L points of silicon, while the difference for the Γ point of diamond is even 0.73 eV. All corrections apparently have the same sign. If RPA screening is used instead (see also Table 4.1), the differences from the standard GW values reduce to roughly 0.3 eV in the case of silicon and to roughly 0.4 eV for diamond. The obvious conclusion is that, if vertex and self-consistency corrections are included to first order, the compensation between them (see also further on) is clearly incomplete.

Table 4.1: GW and $GW+V+SC$ direct gaps (in eV) for RPA screening and RPA+V+SC screening for silicon (Γ , X , and L points) and diamond (Γ point). The LDA direct gaps and experimental data are also given.

Method/Source	Γ	X	L
	silicon		
GW/RPA (standard GW)	3.31	4.20	3.38
$GW/RPA+V+SC$	3.38	4.26	3.44
$GW+V+SC/RPA$	3.58	4.53	3.65
$GW+V+SC/RPA+V+SC$	3.67	4.64	3.77
LDA	2.53	3.35	2.61
Expt.[2, 61]	3.40	4.25	3.45
standard GW literature	3.35[49]	4.43[49]	3.54[49]
	diamond		
GW/RPA (standard GW)	7.63		
$GW/RPA+V+SC$	7.83		
$GW+V+SC/RPA$	8.08		
$GW+V+SC/RPA+V+SC$	8.36		
LDA	5.51		
Expt.[61]	7.3		
standard GW literature	7.5[49];	7.63[73];	7.26[35]

In Table 4.2 details of our calculational results are presented. It is seen that we have concentrated on QP energies of the highest valence band (HVB) and the lowest conduction band (LCB). The highest valence state and lowest conduction state at the Γ point are denoted by Γ'_{25v} and Γ_{15c} , respectively. At the X and L points these states are denoted by X_{4v} , X_{1c} , L_{3v} , and L_{1c} , respectively. We have given for the GW self-energy diagram,

minus v^{XC} , as well as for the respective SC1, SC2, SC3, SC4, and V self-energy diagrams the expectation values together with the related energy derivatives δ . Results are given for both RPA and RPA+V+SC screening, both for silicon and diamond. The calculation of the contribution of the V self-energy correction to the difference in expectation value for LCB and HVB at the Γ point for silicon had already been done in Ref. [13]. However, due to an error in the program code, the result given in Ref. [13] of 0.12 eV is incorrect. The correct value is -0.26 eV; see Table 4.2. Concerning the SC self-energy corrections, one can argue that a GW insertion and a v^{XC} insertion have much in common, such that SC1 and SC2 are likely to compensate partially. It is observed that the SC1 and SC2 self-energy diagrams individually lead to relatively large corrections to the absolute energies of the HVB and LCB and have indeed the tendency to compensate each other, though not completely. The SC3 and SC4 self-energy diagrams are self-energy corrections to the Hartree diagram, in which the valence charge density is corrected to first order in W . As the valence charge density in DFT is equal to the exact density, the first-order corrections to the LDA valence charge density are expected to be minor.[35] It is observed that the contribution to the difference in expectation value for the LCB and HVB due to the SC Hartree diagrams (SC3+SC4) is very small indeed as compared to the contribution due to the SC1+SC2 self-energy diagrams. The difference in expectation value for the LCB and HVB of the V and of the total SC correction can also easily be obtained from the entries in Table 4.2. By doing so, the V correction appears to compensate the SC correction to about 45% in the case of RPA screening and to about 35% in the case of RPA+V+SC screening for silicon. For diamond these percentages are about 15% and -10% , respectively, so that the term compensation is not even appropriate.

The above-mentioned $GW+V+SC/RPA+V+SC$ result is puzzling in a certain sense: If the sum of all first-order corrections to the standard GW gap does not appear to be negligibly small, the question arises which group of diagrams then have to be considered in order to “justify” the standard GW result. Before trying to answer this question it is necessary, however, to be as certain as possible that our calculations do not contain weaknesses of whatever kind. This has led us to the performance of a few checks, which are outlined in the next Section.

4.4 Checks

In this Section we report on a few checks that we have performed concerning the V+SC self-energy corrections. First, for RPA screening, we improved upon the PPM concerning the matrix M in accordance with a proposal of Farid[27], in which he points to the violation of Johnson’s f -sum rule if one sticks to the matrix M of Eq. (4.8). Apart from $P_{\mathbf{G},\mathbf{G}'}(\mathbf{k};\omega = 0)$ we now also have to calculate the leading term of $P_{\mathbf{G},\mathbf{G}'}(\mathbf{k};\omega \rightarrow \infty)$;

see Eq. (4.9). In agreement with Ref. [24], we find that the diagonal elements of the matrix M of Eq. (4.9) are smaller than those given by the Johnson f -sum rule and that the off-diagonal elements deviate even more. When applying the correct matrix M , the standard GW direct band gap of silicon at the Γ point becomes only 0.015 eV smaller, however. In fact, this is not unexpected, as the use of Johnson's f -sum rule (see, for instance, Refs. [49] and [64]) generally leads to excellent agreement between standard GW and experimental gap values. Furthermore, it is also found that the $GW+V+SC/RPA$ direct band gap of silicon at Γ , when calculated with the correct matrix M , stays practically the same: The value becomes only 0.011 eV smaller. It can therefore safely be concluded that the violation of the Johnson f -sum rule yields only insignificant deviations in corrected gap values.

A second point of possible concern is the assumed closeness of LDA wave functions and $GW+V+SC$ wave functions. Though it is demonstrated in Refs. [35] and [49] that the LDA wave functions and the GW wave functions are close, it is not *a priori* certain that this also holds in the presence of the $V+SC$ self-energy corrections. This, however, has to be fulfilled in order to safely apply the expectation value method. We therefore carried through an exact diagonalization procedure for the HVB and LCB at the Γ point of silicon, using RPA screening. In this procedure only coupling between states of equal symmetry needs to be considered, leading, among 65 electron bands, to a 6×6 matrix in the LDA basis to be diagonalized only. In doing so, both the standard GW and the $GW+V+SC/RPA$ direct band gap become larger by an amount of only 0.001 eV compared to the values obtained within the expectation value method. It can therefore also safely be concluded that the LDA wave functions and the $GW+V+SC$ wave functions are sufficiently similar.

A third check concerns the LDA starting point. Though the LDA wave functions are to a large extent similar to the GW wave functions (and to the $GW+V+SC$ wave functions as shown above), the conduction-band energy levels in the LDA are significantly lower than those in GW (and $GW+V+SC$). Though this is generally not thought to be an important issue, we nevertheless would like to investigate whether a LDA input in which the quasiparticle shift is included could improve the results. In a sense such an altered input could be considered to be closer to a " GW set of wave functions with accompanying energy levels" than the usual LDA input. We therefore applied the so-called scissors operator to the LDA by changing the LDA exchange-correlation potential $v^{XC}(\mathbf{k})$ into $v^{XC}(\mathbf{k}) + \Delta \sum_c |c, \mathbf{k}\rangle \langle c, \mathbf{k}|$, where c is meant to indicate conduction bands and $\Delta = 0.8$ eV (for silicon) being about the standard GW conduction-band shift. Leaving the LDA wave functions unaltered, we can now construct another Green's function and insert it into the RPA polarizability, the GW self-energy, and the $V+SC$ self-energy correction. In doing so, the (RPA) dielectric constant changes and becomes equal to 10.9 ($N_{gr} = 6$). The new standard GW direct gap at Γ (of silicon) appears to be about 0.2 eV larger than the value obtained with the LDA as the starting point, while the new $GW+V+SC/RPA$ direct gap is about 0.1 eV larger than before. It therefore shows that this kind of change in the LDA

starting point in the GW type of calculations does not improve things. Incidentally, the dependence on starting point Hamiltonians for GW or related types of calculations and, more specifically, the apparent preference for the LDA starting point are interesting in themselves and not sufficiently settled in our opinion.

4.5 Discussion on the self-consistency self-energy diagrams

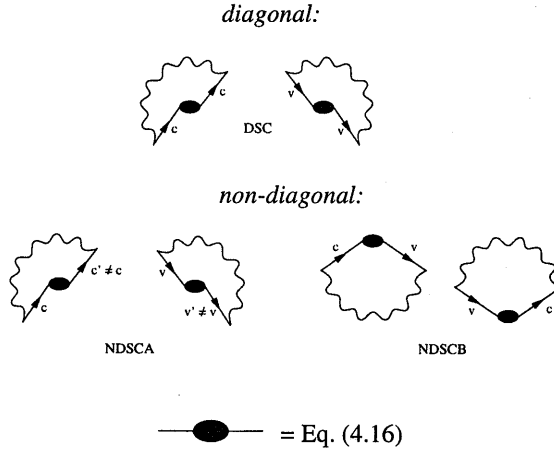


Figure 4.5: $SC1+SC2$ self-energy correction subdiagrams with diagonal and nondiagonal GW self-energy insertions in the LDA basis. The former subdiagrams are indicated with DSC and the latter subdiagrams are indicated with $NDSCA$ and $NDSCB$. Time increases from bottom to top. v stands for a valence-band index and c stands for a conduction-band index (which have to be summed over). In the case of DSC the band indices on both sides of the ellipse are identical.

If we, in spite of the latter discussion, nevertheless pursue the issue of LDA wave functions and GW wave functions being highly similar, it is tempting to subdivide the $SC1+SC2$ self-energy subdiagrams. To this end we give the expression for the insertion, in the LDA basis, occurring in the $SC1+SC2$ self-energy correction to the LDA energy $\varepsilon_l(\mathbf{k})$ (the electron bands l' and l'' are summation variables and the energy ω and the wave vector \mathbf{q} are integration variables):

$$\langle l', \mathbf{q} + \mathbf{k} | \hbar \Sigma^{GW}(\mathbf{q} + \mathbf{k}; \omega + \varepsilon_l(\mathbf{k})) - v^{XC}(\mathbf{q} + \mathbf{k}) | l'', \mathbf{q} + \mathbf{k} \rangle. \quad (4.16)$$

The SC1+SC2 self-energy subdiagrams can be subdivided into the “diagonal SC” (DSC) and “nondiagonal SC” (NDSC) groups of subdiagrams of Fig. 4.5. The reason for doing this is that the DSC group of subdiagrams consists of subdiagrams in which the insertion, given by Eq. (4.16), is taken between *the same* conduction (*c*) or valence (*v*) states only. The NDSC group of subdiagrams can further be subdivided into the NDSCA and NDSCB groups of subdiagrams; see Fig. 4.5. The NDSCA and NDSCB groups of subdiagrams are initially expected to be small, the reason being that in these latter subdiagrams the insertion, given by Eq. (4.16), is taken between *different* states. If we simply ignore the NDSC contribution and calculate the difference between the *GW*+DSC/RPA and the standard *GW* gap value, applying the expectation value method using standard *GW* energy derivatives δ , we obtain the values 0.32, 0.49, and 0.40, and 0.34 eV, for the Γ , *X*, and *L* points of silicon and the Γ point of diamond, respectively. Considering the fact that the vertex correction *V* to the self-energy yields a gap correction of about -0.3 eV for silicon and about -0.1 eV for diamond (see Table 4.2), we would then find that the totality of the *V* plus DSC correction appears to be minor for silicon, while the compensation is less pronounced for diamond. Unfortunately, however, our *actual* results on the group of NDSC subdiagrams do not confirm the above reasoning at all. It is true that we find the contribution to the gap due to the NDSCA group of Fig. 4.5 to be very small, but, unfortunately, this does not hold for the remaining group of subdiagrams, NDSCB. The discrepancy between the actual contribution of the NDSC subdiagrams and our above reasoning (expecting them to be insignificant), however, can be understood as follows. Taking the square of the matrix elements $\langle l, \mathbf{k} | \hbar \Sigma^{GW}(\mathbf{k}; \varepsilon_l(\mathbf{k})) - v^{XC}(\mathbf{k}) | l', \mathbf{k} \rangle$, the nondiagonal ($l \neq l'$) values are found to be about two orders of magnitude smaller than the diagonal ($l = l'$) ones. This is one of the reasons for the correction[35]

$$\sum_{l' \neq l} \frac{|\langle l, \mathbf{k} | \hbar \Sigma^{GW}(\mathbf{k}; \varepsilon_l(\mathbf{k})) - v^{XC}(\mathbf{k}) | l', \mathbf{k} \rangle|^2}{\varepsilon_l(\mathbf{k}) - \varepsilon_{l'}(\mathbf{k})} \quad (4.17)$$

to the QP energies to be very small, which is related to the high similarity of the *GW* and LDA wave functions. On the other hand, in order to calculate the SC1+SC2 self-energy contribution the matrix element itself is required, instead of its square. Furthermore, the energy denominators pertaining to the NDSCB subdiagrams contain one energy difference consisting only of electron energies, while in the case of the DSC (and NDSCA) subdiagrams each energy difference contains a plasmon energy (which is relatively large).

4.6 A remarkable cancellation

We note that it is possible to view upon the orders in *W* in a different way by expanding the wave-function renormalization factor $Z_{l,\mathbf{k}}$ occurring in Eq. (4.13). *Z* can formally be

written as

$$Z_{l,\mathbf{k}} = 1 + \sum_{n=1}^{\infty} \left\{ \hbar \langle l, \mathbf{k} | \frac{\partial \Sigma(\mathbf{k}; \omega)}{\partial \omega} \Big|_{\omega = \varepsilon_l(\mathbf{k})} | l, \mathbf{k} \rangle \right\}^n \quad (4.18)$$

such that, in fact, an infinite number of higher-order terms in W are involved via the energy derivative of Σ . In doing so, we observe a remarkable cancellation between corrections to the band gap due to the V and SC corrections to the self-energy Σ on the one hand and corrections to the band gap due to the energy dependence of Σ^{GW} on the other hand. A cancellation of this particular kind has been reported by van Haeringen for both the Bloch-Nordsieck model describing electron-photon coupling [12, 39] and the Fröhlich polaron model describing electron-phonon coupling [40]. A cancellation between self-consistency corrections to Σ and the energy dependence of Σ was indicated by DuBois[22] and also mentioned by Rice[72].

In order to be able to present the cancellation effect, it is necessary to return to the expectation value method that was introduced in Section 4.2. We expand the right-hand side (RHS) of Eq. (4.13) to second order in the screened interaction W by making a Taylor expansion of the denominator containing the energy derivative and the resulting expression for the quasiparticle energy $E_l^{QP}(\mathbf{k})$ is

$$\begin{aligned} E_l^{QP}(\mathbf{k}) \approx & \varepsilon_l(\mathbf{k}) + \langle l, \mathbf{k} | \hbar \Sigma^{GW}(\mathbf{k}; \varepsilon_l(\mathbf{k})) - v^{XC}(\mathbf{k}) | l, \mathbf{k} \rangle + \\ & \langle l, \mathbf{k} | \hbar \Sigma^{GW}(\mathbf{k}; \varepsilon_l(\mathbf{k})) - v^{XC}(\mathbf{k}) | l, \mathbf{k} \rangle \times \delta_l^{GW}(\mathbf{k}) + \\ & \hbar \langle l, \mathbf{k} | \Sigma^{V+SC}(\mathbf{k}; \varepsilon_l(\mathbf{k})) | l, \mathbf{k} \rangle. \end{aligned} \quad (4.19)$$

We have regrouped our calculational results in accordance with Eq. (4.19), taking care of correction terms in the “appropriate order” for both RPA and RPA+V+SC screening. In doing so, note that the convention of viewing upon orders in W is now different from before: The GW expectation value is of “first order” in W , the V+SC self-energy expectation value is of “second order” in W , and the GW expectation value times its energy derivative is also of “second order” in W . The above-mentioned cancellation effect concerns the last two terms on the RHS of Eq. (4.19). In Table 4.3 we present the values of these terms for the HVB and LCB of the Γ , X , and L points of silicon and for the Γ point of diamond, which can be produced with the data given in Table 4.2. It is observed that no cancellation occurs for the LCB and HVB separately. A remarkable cancellation is seen to occur, however, for the band-gap values, in all cases leading to a gap contribution smaller than 0.1 eV. It should be noted in this connection that a similar result has already been obtained in the case of the quasi-one-dimensional semiconducting wire; see Ref. [38].

It will be clear that this result does not as yet contribute to a deeper understanding of the celebrated standard GW result. This particular cancellation causes the GW +V+SC energies to be equal to the LDA energies plus the GW self-energy expectation values calculated at the LDA energy. This is puzzling since in the case of the GW gap, calculating

the GW self-energy expectation value at the LDA energy instead of at the GW energy, the energy derivative was absolutely required to obtain agreement with experiment. The cancellation rather points to the existence of an apparent “sum rule”, which unfortunately is unexplained as yet. There is a possible connection to Ward identities[80], but no reference to a specific Ward identity has been discussed in the literature. If, in our case, an identity of the above kind indeed exists, the above results could presumably be considered as an internal check on the correctness of our calculations rather than contributing to the identification of the relevant group of diagrams that leads to the same gap results as standard GW .

4.7 Discussion and conclusions

The present work was motivated by the idea that the apparent success of standard GW in predicting electronic properties could possibly be supported by a compensation between first-order vertex and self-consistency corrections to the band gap of silicon and diamond. Compensations of this type are occasionally reported on in the literature, mainly in the case of the homogeneous electron gas, but also in the case of a quasi-one-dimensional semi-conducting wire. It seemed of interest to investigate to what extent such a compensation can also be found for a completely realistic case. The starting point has been a fully converged LDA calculation for both silicon and diamond. Our effort has been to calculate the contribution of complete sets of subdiagrams contributing to both the polarizability P (to first order in W) and the self-energy Σ (to second order in W). We found large compensations between the first-order vertex and self-consistency corrections to P , but the result concerning Σ and the related gap value is disappointing in the sense that there appears to be only a 35% compensation between the V and SC self-energy corrections (to the difference in their expectation value for the LCB and HVB) in the case of silicon, while such a compensation is in fact absent in the case of diamond. The resulting corrected gap values appear to be about 0.4 eV and 0.7 eV larger than the standard GW values for silicon and diamond, respectively. This result does therefore not give the expected help in understanding the success of the standard GW approach. In view of this more or less unexpected result, much effort has been put in checking the correctness of a large number of computational steps, such that we are convinced of the correctness of our final results. Furthermore, by expanding the wave-function renormalization function, we have found a cancellation of particular correction terms occurring for the $GW+V+SC$ gap. It is therefore worthwhile to speculate on other more refined compensating mechanisms that possibly could explain the “correctness” of standard GW . In this connection we recall the work of Shirley[76], briefly discussed in earlier Sections, from which it could be deduced that a possibly more complete compensation could be obtained if we would be able to evaluate self-consistently the sum of the GW self-energy diagram and the vertex correction diagram.

In 1965 Hedin[44] already put forward that corrections to standard GW should preferably be included by using a self-consistent G . Unfortunately, this is a tremendous task, even for the homogeneous electron gas, but in our opinion its performance for silicon and diamond is considered to be crucial as it could very well contribute to a better understanding of the success of the standard GW approach for these latter materials.

Table 4.2: Expectation values of the first-order self-consistency and vertex self-energy corrections, with RPA and RPA+V+SC screening, for the HVB and LCB of the Γ , X , and L points of silicon (in eV). Their energy derivatives δ are given in parentheses (— means zero energy derivative). The expectation values and energy derivatives of the GW self-energy minus v^{XC} are also given; see column 2.

l, \mathbf{k}	$GW - v^{\text{XC}}$	SC1	SC2	SC3	SC4	Total SC	V	Total V+SC
silicon: RPA screening								
Γ'_{25v}	-1.211 (-0.288)	-3.652 (0.231)	3.513 (-0.147)	1.287 (—)	-1.152 (—)	-0.004 (0.084)	0.076 (-0.088)	0.072 (-0.004)
Γ_{15c}	-0.203 (-0.286)	-2.180 (-0.130)	2.734 (0.197)	0.441 (—)	-0.396 (—)	0.599 (0.067)	-0.181 (-0.079)	0.418 (-0.012)
X_{4v}	-1.283 (-0.315)	-3.744 (0.338)	3.424 (-0.237)	0.792 (—)	-0.706 (—)	-0.234 (0.101)	0.158 (-0.079)	-0.075 (0.021)
X_{1c}	-0.159 (-0.261)	-1.688 (-0.101)	2.174 (0.161)	-0.077 (—)	0.068 (—)	0.477 (0.060)	-0.162 (-0.070)	0.314 (-0.010)
L'_{3v}	-1.254 (-0.299)	-3.675 (0.284)	3.468 (-0.194)	1.074 (—)	-0.957 (—)	-0.090 (0.091)	0.130 (-0.089)	0.040 (0.002)
L_{1c}	-0.246 (-0.273)	-2.211 (-0.123)	2.720 (0.187)	0.587 (—)	-0.524 (—)	0.572 (0.064)	-0.193 (-0.076)	0.378 (-0.011)
silicon: RPA+V+SC screening								
Γ'_{25v}	-1.310 (-0.290)	-3.654 (0.226)	3.526 (-0.140)	1.292 (—)	-1.152 (—)	0.012 (0.086)	0.017 (-0.092)	0.030 (-0.006)
Γ_{15c}	-0.217 (-0.288)	-2.209 (-0.125)	2.755 (0.193)	0.444 (—)	-0.396 (—)	0.594 (0.068)	-0.181 (-0.084)	0.413 (-0.016)
X_{4v}	-1.365 (-0.317)	-3.710 (0.325)	3.407 (-0.222)	0.805 (—)	-0.706 (—)	-0.204 (0.103)	0.073 (-0.082)	-0.131 (0.020)
X_{1c}	-0.161 (-0.263)	-1.692 (-0.090)	2.163 (0.150)	-0.078 (—)	0.068 (—)	0.461 (0.060)	-0.130 (-0.072)	0.331 (-0.012)
L'_{3v}	-1.347 (-0.301)	-3.643 (0.271)	3.455 (-0.179)	1.091 (—)	-0.957 (—)	-0.054 (0.093)	0.036 (-0.091)	-0.019 (0.001)
L_{1c}	-0.257 (-0.275)	-2.215 (-0.111)	2.708 (0.176)	0.597 (—)	-0.524 (—)	0.566 (0.065)	-0.168 (-0.078)	0.398 (-0.013)

Table 4.2: continued; for the HVB and LCB of the Γ point of diamond.

l, \mathbf{k}	$GW - v^{XC}$	SC1	SC2	SC3	SC4	Total SC	V	Total V+SC
diamond: RPA screening								
Γ'_{25v}	-2.083 (-0.191)	-3.666 (0.128)	3.524 (-0.085)	1.725 (-)	-1.543 (-)	0.040 (0.043)	0.109 (-0.036)	0.149 (0.007)
Γ_{15c}	0.445 (-0.187)	-2.305 (-0.062)	2.853 (0.099)	1.055 (-)	-0.956 (-)	0.647 (0.036)	0.019 (-0.032)	0.666 (0.005)
diamond: RPA+V+SC screening								
Γ'_{25v}	-2.321 (-0.194)	-3.696 (0.125)	3.567 (-0.081)	1.776 (-)	-1.543 (-)	0.104 (0.044)	-0.013 (-0.041)	0.091 (0.003)
Γ_{15c}	0.459 (-0.191)	-2.356 (-0.058)	2.889 (0.096)	1.091 (-)	-0.956 (-)	0.668 (0.039)	0.041 (-0.037)	0.709 (0.002)

Table 4.3: Correction contributions due to the last two terms on the RHS of Eq. (4.19) for the HVB and LCB of silicon and diamond (in eV), in the case of RPA screening and RPA+V+SC screening (for the latter case the values are given in parentheses). With $\langle GW - v^{XC} \rangle$ we mean $\langle l, \mathbf{k} | \hbar \Sigma^{GW}(\mathbf{k}; \varepsilon_l(\mathbf{k})) - v^{XC}(\mathbf{k}) | l, \mathbf{k} \rangle$ and with $\langle V + SC \rangle$ we mean $\hbar \langle l, \mathbf{k} | \Sigma^{V+SC}(\mathbf{k}; \varepsilon_l(\mathbf{k})) | l, \mathbf{k} \rangle$.

l, \mathbf{k}	$\langle GW - v^{XC} \rangle \times \delta_l^{GW}(\mathbf{k})$	$\langle V+SC \rangle$	Total	Gap contribution
silicon				
Γ'_{25v}	0.349 (0.380)	0.072 (0.030)	0.421 (0.410)	
Γ_{15c}	0.058 (0.062)	0.418 (0.413)	0.476 (0.475)	0.055 (0.065)
X_{4v}	0.404 (0.433)	-0.075 (-0.131)	0.329 (0.302)	
X_{1c}	0.041 (0.042)	0.314 (0.331)	0.355 (0.373)	0.026 (0.071)
L'_{3v}	0.375 (0.405)	0.040 (-0.019)	0.415 (0.386)	
L_{1c}	0.067 (0.071)	0.378 (0.398)	0.445 (0.469)	0.030 (0.083)
diamond				
Γ'_{25v}	0.398 (0.450)	0.149 (0.091)	0.547 (0.541)	
Γ_{15c}	-0.083 (-0.088)	0.666 (0.709)	0.583 (0.621)	0.036 (0.080)

Appendix A: The expression for a polarizability correction subdiagram

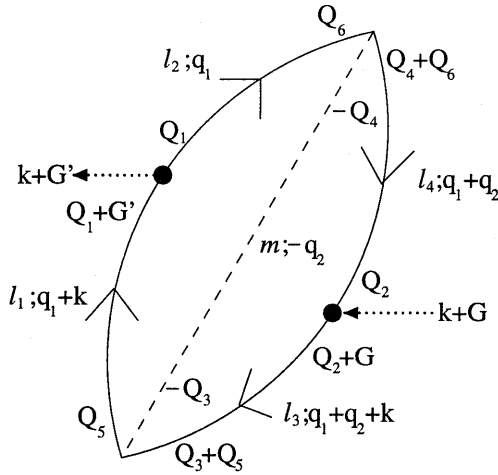


Figure A.1: Vertex correction subdiagram included in the correction to the polarizability $P_{\mathbf{G}, \mathbf{G}'}(\mathbf{k}; \omega)$. A directed line denotes the LDA Green's function G^0 , and the dashed line stands for W^{scr} [see Eq. (4.2)]. The two dotted, arrowed lines with $\mathbf{k} + \mathbf{G}$ and $\mathbf{k} + \mathbf{G}'$ indicate the two crystal momenta for which the correction ΔP is taken. The meaning of the labels is explained in the main text.

In this appendix we give the worked-out algebraic expression for a vertex correction subdiagram of the polarizability in the momentum representation; see Fig. A.1. The momentum flow through the subdiagram can be deduced using momentum conservation at the interaction vertices. The evaluation of this particular correction entails summations

over conduction bands (l_1 and l_2), valence bands (l_3 and l_4), plasmon bands (m), and reciprocal lattice vectors $\mathbf{Q}_1 - \mathbf{Q}_6$. The presence of reciprocal lattice vectors is due to the interaction of an electron or hole with the ion lattice. Furthermore, the evaluation of this correction involves an integration over the reduced wave vectors \mathbf{q}_1 and \mathbf{q}_2 . As mentioned in section 4.2, one integration can be performed over $\mathcal{I}_{\mathbf{k}}$. The expression is:

$$\begin{aligned}
 \Delta P_{\mathbf{G}, \mathbf{G}'}(\mathbf{k}; \omega) = & -2 \int_{\text{1BZ}} \frac{d^3 q_1}{(2\pi)^3} \int_{\text{1BZ}} \frac{d^3 q_2}{(2\pi)^3} \sum_{l_1 \in c} \sum_{l_2 \in c} \sum_{l_3 \in v} \sum_{l_4 \in v} \sum_m \\
 & \left(\sum_{\mathbf{Q}_1} d_{l_1, \mathbf{q}_1 + \mathbf{k}}^0(\mathbf{Q}_1 + \mathbf{G}') d_{l_2, \mathbf{q}_1}^{0*}(\mathbf{Q}_1) \right) \left(\sum_{\mathbf{Q}_2} d_{l_4, \mathbf{q}_1 + \mathbf{q}_2}^0(\mathbf{Q}_2) d_{l_3, \mathbf{q}_1 + \mathbf{q}_2 + \mathbf{k}}^{0*}(\mathbf{Q}_2 + \mathbf{G}) \right) \\
 & \times \left(\sum_{\mathbf{Q}_5} d_{l_1, \mathbf{q}_1 + \mathbf{k}}^{0*}(\mathbf{Q}_5) \sum_{\mathbf{Q}_3} d_{l_3, \mathbf{q}_1 + \mathbf{q}_2 + \mathbf{k}}^0(\mathbf{Q}_3 + \mathbf{Q}_5) w_{m, -\mathbf{q}_2}(-\mathbf{Q}_3) \right) \\
 & \times \left(\sum_{\mathbf{Q}_6} d_{l_2, \mathbf{q}_1}^0(\mathbf{Q}_6) \sum_{\mathbf{Q}_4} d_{l_4, \mathbf{q}_1 + \mathbf{q}_2}^{0*}(\mathbf{Q}_4 + \mathbf{Q}_6) w_{m, -\mathbf{q}_2}^*(-\mathbf{Q}_4) \right) \\
 & \times \left[[\omega_m(-\mathbf{q}_2) + \varepsilon_{l_1}(\mathbf{q}_1 + \mathbf{k}) - \varepsilon_{l_3}(\mathbf{q}_1 + \mathbf{q}_2 + \mathbf{k})][\omega_m(-\mathbf{q}_2) + \varepsilon_{l_2}(\mathbf{q}_1) - \varepsilon_{l_4}(\mathbf{q}_1 + \mathbf{q}_2)] \right. \\
 & \times \left. [\omega - \omega_m(-\mathbf{q}_2) - \varepsilon_{l_1}(\mathbf{q}_1 + \mathbf{k}) + \varepsilon_{l_4}(\mathbf{q}_1 + \mathbf{q}_2)] \right]^{-1}. \quad (\text{A.1})
 \end{aligned}$$

Here ε_l are LDA energies and d_l^0 are LDA plane-wave coefficients; ω_m are PPM energies and w_m are PPM coefficients. c and v denote the conduction bands and valence bands, respectively. The factor 2 originates from summation over spins. In this particular example given by Eq. (A.1), the head element ($\mathbf{G} = \mathbf{0}, \mathbf{G}' = \mathbf{0}$) for $\mathbf{k} \rightarrow \mathbf{0}$ has a constant contribution if $l_1 = l_2$ and $l_3 = l_4$, because then we have twice an inner product of a wavefunction with itself, which is unity. The head element also has linear contributions in \mathbf{k} for $\mathbf{k} \rightarrow \mathbf{0}$ if $l_1 \neq l_2$ or $l_3 \neq l_4$. Also the wing elements ($\mathbf{G} = \mathbf{0}$ or $\mathbf{G}' = \mathbf{0}$) have a constant contribution. The energy denominator contains products of energy differences. For this particular correction to the polarizability given by Eq. (A.1) the energy denominator consists of three such energy differences.

For $\omega = 0$ there are no vanishing energy denominators for any subdiagram contributing to the polarizability P .

Bibliography

- [1] F. Aryasetiawan and O. Gunnarsson, Rep. Prog. Phys. **61**, 237 (1998).
- [2] D.E. Aspnes and A.A. Studna, Phys. Rev. B **27**, 985 (1983).
- [3] G.B. Bachelet, H.S. Greenside, G.A. Baraff, and M. Schlüter, Phys. Rev. B **24**, 4745 (1981).
- [4] W.H. Backes, P.A. Bobbert, and W. van Haeringen, Phys. Rev. B **49**, 7564 (1994).
- [5] W.H. Backes, P.A. Bobbert, and W. van Haeringen, Phys. Rev. B **51**, 4950 (1995).
- [6] W.H. Backes, F.C. de Nooij, P.A. Bobbert, and W. van Haeringen, Physica B (Amsterdam) **217**, 207 (1996).
- [7] W.H. Backes, *On the band gap variation in SiC polytypes*, Ph.D. thesis, Eindhoven University of Technology (1996).
- [8] G. Baldini and B. Bosacchi, Phys. Stat. Sol. **38**, 325 (1970).
- [9] U. von Barth and B. Holm, Phys. Rev. B **54**, 8411 (1996); B. Holm and U. von Barth, *ibid.* **57**, 2108 (1998).
- [10] G. Baym and L.P. Kadanoff, Phys. Rev. **124**, 287 (1961); G. Baym *ibid.* **127**, 1391 (1962).
- [11] F. Bechstedt, P. Käckell, A. Zywietz, K. Karch, B. Adolph, K. Tenelsen, and J. Furthmüller, Phys. Status Solidi B **202**, 35 (1997).
- [12] F. Bloch and A. Nordsieck, Phys. Rev. **52**, 54 (1937).
- [13] P.A. Bobbert and W. van Haeringen, Phys. Rev. B **49**, 7564 (1994).
- [14] F. Brosens, L.F. Lemmens, and J.T. Devreese, Phys. Stat. Sol. B **74**, 45 (1976).
- [15] P.E. van Camp, V.E. van Doren, and J.T. Devreese, Phys. Rev. B **24**, 1096 (1981).
- [16] J. Chen, Z.H. Levine, and J.W. Wilkins, Phys. Rev. B **50**, 11 514 (1994).
- [17] W.J. Choyke, D.R. Hamilton, and L. Patrick, Phys. Rev. **133**, A1163 (1964).
- [18] R. Daling and W. van Haeringen, Phys. Rev. B **40**, 11 659 (1989).
- [19] R. Daling, P. Unger, P. Fulde, and W. van Haeringen, Phys. Rev. B **43**, 1851 (1991).

- [20] R. Del Sole, L. Reining, and R.W. Godby, Phys. Rev. B **49**, 8024 (1994).
- [21] P.A.M. Dirac, *The principles of quantum mechanics*, 4th rev. ed. (Clarendon Press, Oxford, 1967).
- [22] D.F. DuBois, Ann. Phys. (N.Y.) **7**, 174 (1959); **8**, 24 (1959).
- [23] G.B. Dubrovskii and V.I. Sankin, Sov. Phys. Solid State **17**, 1847 (1975).
- [24] G.E. Engel and B. Farid, Phys. Rev. B **46**, 15 812 (1992).
- [25] G.E. Engel and B. Farid, Phys. Rev. B **47**, 15 931 (1993).
- [26] B. Farid, *Towards ab initio calculation of electron energies in semiconductors*, Ph.D. thesis, Eindhoven University of Technology (1989).
- [27] B. Farid (private communication).
- [28] R.A. Faulkner, Phys. Rev. **184**, 713 (1969); H.W. Icenogle, B.C. Platt, and W.L. Wolfe, Appl. Opt. **15**, 2348 (1976).
- [29] A.L. Fetter and J.D. Walecka, *Quantum Theory of Many-Particle Systems* (McGraw-Hill, New York, 1971).
- [30] V. Fock, Z. Phys. **61**, 126 (1930).
- [31] D.J.W. Geldart and R. Taylor, Can. J. Phys. **48**, 155; 167 (1970).
- [32] M. Gell-Mann and K.A. Brueckner, Phys. Rev. **106**, 364 (1957).
- [33] M. Gell-Mann, Phys. Rev. **106**, 369 (1957).
- [34] R.W. Godby, M. Schlüter, and L.J. Sham, Phys. Rev. Lett. **56**, 2415 (1986); Phys. Rev. B **35**, 4170 (1987).
- [35] R.W. Godby, M. Schlüter, and L.J. Sham, Phys. Rev. B **37**, 10 159 (1988).
- [36] H.J. de Groot, P.A. Bobbert, and W. van Haeringen, Phys. Rev. B **52**, 11 000 (1995).
- [37] H.J. de Groot, R.T.M. Ummels, P.A. Bobbert, and W. van Haeringen, Phys. Rev. B **54**, 2374 (1996).
- [38] H.J. de Groot, *Effects of self-consistency and vertex corrections on the GW-gap of semiconductors: a model study*, Ph.D. thesis, Eindhoven University of Technology (1996).

- [39] W. van Haeringen, *Physica (Amsterdam)* **26**, 289 (1960).
- [40] W. van Haeringen, *Phys. Rev.* **137**, A1902 (1965).
- [41] W. van Haeringen, P.A. Bobbert, and W.H. Backes, *Phys. Status Solidi B* **202**, 63 (1997).
- [42] W. Hanke and L.J. Sham, *Phys. Rev. B* **12**, 4501 (1975).
- [43] D.R. Hartree, *Proc. Cambr. Philos. Soc.* **24**, 89 (1928).
- [44] L. Hedin, *Phys. Rev.* **139**, A796 (1965).
- [45] L. Hedin and B.I. Lundqvist, *J. Phys. C* **4**, 2064 (1971).
- [46] P. Hohenberg and W. Kohn, *Phys. Rev.* **136**, B864 (1964).
- [47] J. Hubbard, *Proc. R. Soc. London, Ser. A* **243**, 336 (1957).
- [48] M.S. Hybertsen and S.G. Louie, *Phys. Rev. B* **32**, 7005 (1985); *Phys. Rev. Lett.* **55**, 1418 (1985).
- [49] M.S. Hybertsen and S.G. Louie, *Phys. Rev. Lett.* **55**, 1418 (1985); *Phys. Rev. B* **34**, 5390 (1986).
- [50] M.S. Hybertsen and S.G. Louie, *Phys. Rev. B* **35**, 5585 (1987).
- [51] D.L. Johnson, *Phys. Rev. B* **9**, 4475 (1974).
- [52] R.O. Jones and O. Gunnarsson, *Rev. Mod. Phys.* **61**, 689 (1989).
- [53] P. Käckell, B. Wenzien, and F. Bechstedt, *Phys. Rev. B* **50**, 10 761 (1994).
- [54] K. Karch, F. Bechstedt, P. Pavone, and D. Strauch, *Phys. Rev. B* **53**, 13 400 (1996).
- [55] C. Kittel, *Introduction to Solid State Physics*, 5th ed. (Wiley, New York, 1976), page 309.
- [56] W. Knorr and R.W. Godby, *Phys. Rev. Lett.* **68**, 639 (1992).
- [57] W. Knorr and R.W. Godby, *Phys. Rev. B* **50**, 1779 (1994).
- [58] W. Kohn, *Phys. Rev.* **110**, 857 (1958).
- [59] W. Kohn and L.J. Sham, *Phys. Rev.* **140**, A1133 (1965).

- [60] W.R.L. Lambrecht, S. Limpijumnong, S.N. Rashkeev, and B. Segall, *Phys. Status Solidi B* **202**, 5 (1997).
- [61] Landolt-Börnstein, *Semiconductors: Physics of Group IV Elements and III-V Compounds*, edited by K.-H. Hellwege and O. Madelung, New Series, Group III, Vol. 17, Pt. a (Springer-Verlag, Berlin, 1982); *ibid.* Vol. 22, Pt. a (Springer-Verlag, Berlin, 1987).
- [62] T. Lei, T.D. Moustakas, R.J. Graham, Y. He, and S.J. Berkowitz, *J. Appl. Phys.* **71**, 4933 (1992); T. Lei, M. Fanciulli, R.J. Molnar, T.D. Moustakas, R.J. Graham, and J. Scanlon, *Appl. Phys. Lett.* **59**, 944 (1992); C.R. Eddy, T.D. Moustakas, and J. Scanlon, *J. Appl. Phys.* **73**, 448 (1993).
- [63] H.H. Li, *J. Phys. Chem. Ref. Data* **9**, 561 (1980).
- [64] W. von der Linden and P. Horsch, *Phys. Rev. B* **37**, 8351 (1988).
- [65] G.D. Mahan and B.E. Sernelius, *Phys. Rev. Lett.* **62**, 2718 (1989).
- [66] R.D. Mattuck, *A Guide to Feynman Diagrams in the Many-Body Problem*, (McGraw-Hill, New York, 1967).
- [67] J.D. Pack and H.J. Monkhorst, *Phys. Rev. B* **16**, 1748 (1977).
- [68] L. Patrick, D.R. Hamilton, and W.J. Choyke, *Phys. Rev.* **143**, 526 (1966).
- [69] J.P. Perdew and A. Zunger, *Phys. Rev. B* **23**, 5048 (1981).
- [70] J.C. Phillips, *Phys. Rev. Lett.* **20**, 550 (1968).
- [71] H. Raether, *Excitation of Plasmons and Interband Transitions by Electrons*, edited by G. Höhler, Springer Tracts in Modern Physics Vol. 88 (Springer, Berlin, 1980).
- [72] T.M. Rice, *Ann. Phys. (N.Y.)* **31**, 100 (1965).
- [73] M. Rohlfing, P. Krüger, and J. Pollmann, *Phys. Rev. B* **48**, 17 791 (1993).
- [74] A. Rubio, J.L. Corkill, M.L. Cohen, E.L. Shirley, and S.G. Louie, *Phys. Rev. B* **48**, 11 810 (1993).
- [75] V.I. Sankin, *Sov. Phys. Solid State* **17**, 1191 (1975).
- [76] E.L. Shirley, *Phys. Rev. B* **54**, 7758 (1996).
- [77] J.C. Slater, *Phys. Rev.* **35**, 210 (1930).

Bibliography

- [78] R.T.M. Ummels, P.A. Bobbert, and W. van Haeringen, *Phys. Rev. B* **57**, 11 962 (1998).
- [79] R.T.M. Ummels, P.A. Bobbert, and W. van Haeringen, *Phys. Rev. B* **58**, 6795 (1998).
- [80] J.C. Ward, *Phys. Rev.* **78**, 182 (1950).
- [81] B. Wenzien, P. Käckell, F. Bechstedt, and G. Cappellini, *Phys. Rev. B* **52**, 10 897 (1995); B. Wenzien, G. Cappellini, and F. Bechstedt, *ibid.* **51**, 14 701 (1995).
- [82] G.C. Wick, *Phys. Rev.* **80**, 268 (1950).
- [83] E.P. Wigner, *Phys. Rev.* **46**, 1002 (1934).
- [84] S.B. Zhang, D. Tomanék, M.L. Cohen, S.G. Louie, and M.S. Hybertsen, *Phys. Rev. B* **40**, 3162 (1989).
- [85] X. Zhu and S.G. Louie, *Phys. Rev. B* **43**, 14 142 (1991).

Dankwoord

Tenslotte wil ik deze pagina gebruiken om collega's en anderen te noemen. Hoewel ik alleen mijn eigen naam op de omslag van dit proefschrift heb vermeld, ben ik deze mensen bijzonder dankbaar voor hun bijdragen aan dit proefschrift. Om te beginnen wil ik mijn promotor Wim van Haeringen bedanken voor zijn begeleiding van mijn promotie, speciaal ook voor zijn voortreffelijke hulp bij het schrijven van de artikelen en dit proefschrift. Copromotor Peter Bobbert wil ik evenzo bedanken, speciaal ook voor zijn wetenschappelijke kennis waarvan ik dankbaar vaak gebruik heb mogen maken. Tweede promotor Thijs Michels wil ik bedanken voor het kritisch lezen van dit proefschrift. Verder bedank ik mijn collega's, te weten Herman de Groot, Walter Backes en Jan-Willem van de Horst voor hun prettige aanwezigheid en Herman daarbij ook voor zijn computertechnische hulp en Walter voor zijn hulp bij de berekeningen aan SiC. Ook bedank ik de overigen in het Werkverband Theoretische Natuurkunde, met name Ria Coopmans-van Basten voor onder andere de thee in de pauzes en Ard-Jan Moerdijk voor zijn computertechnische hulp. De helaas overleden Piet van Camp ben ik nog bijzonder dankbaar voor zijn hulp bij de voorbereidende LDA berekeningen aan SiC. Voor alle hulp bij mijn werkzaamheden op supercomputers bedank ik Arjeh Tal, Bert van Corler van SARA en Patrick Aerts van NCF. En tenslotte gaat mijn dank uit naar de interieurverzorgsters, de kantinejuffrouwen, de medewerkers bij bibliotheek en personeelszaken en de portiers/conciërges van het Natuurkunde gebouw.

Stellingen

behorende bij het proefschrift

GW and beyond: application to SiC, Si, C

van

R.T.M. Ummels

Eindhoven, 27 oktober 1998

I.

De experimentele waarden voor de bandgap van hexagonale polytypen van de halfgeleider silicium-carbide worden uitstekend gereproduceerd in het kader van de *GW*-theorie.

[1] Dit proefschrift, Hoofdstuk 3.

II.

In het geval van de halfgeleider silicium en isolator diamant compenseren de laagste orde correcties op de statische RPA polariseerbaarheid elkaar voor een zeer groot gedeelte. Daarentegen compenseren de laagste orde correcties op de *GW* zelfenergie elkaar niet in voldoende mate voor deze materialen, wat zich uit in relatief grote bijdragen tot hun berekende bandgaps.

[1] Dit proefschrift, Hoofdstuk 4.

III.

De door Pack en Monkhorst gegeven definitie voor de irreducibele zone van de hexagonale Brillouin zone is niet helemaal juist. Deze moet luiden:

$$0 \leq 2u_p + u_r \leq 1, \quad 0 \leq u_r \leq u_p \leq \frac{1}{2}, \quad 0 \leq u_s \leq \frac{1}{2}.$$

[1] J.D. Pack en H.J. Monkhorst, Phys. Rev. B **16**, 1748 (1977).

IV.

Aan de in de literatuur aanvaarde experimentele waarde voor de energie van de laagste geleidingsband in het *L* punt van kubisch silicium-carbide moet op grond van verschillende *ab-initio GW* berekeningen getwijfeld worden.

[1] W.H. Backes, proefschrift TUE 1996; M. Rohlfing, P. Krüger en J. Pollmann, Phys. Rev. B **48**, 17791 (1993); B. Wenzien, P. Käckell, F. Bechstedt en G. Cappellini, Phys. Rev. B **52**, 10897 (1995).

[2] Landolt-Börnstein, *Semiconductors: Physics of Group IV Elements and III-V Compounds*, bewerkt door K.-H. Hellwege en O. Madelung, New Series, Group III, Vols. 17 en 22, Pt. a (Springer-Verlag, Berlin, 1982 en 1987).

V.

In tegenstelling tot DFT-LDA en Hartree-Fock berekeningen, maakt het bij *GW* berekeningen van de bandgap van polymeren veel uit of er een enkele keten dan wel een drie-dimensionaal kristal wordt beschouwd; in het eerste geval resulteert een veel grotere bandgap.

VI.

De door Enderlein *et al.* gesuggereerde analogie tussen de theorie van gatengassen in III-V halfgeleiders, waarbij men lichte en zware gaten kan onderscheiden, en de thermodynamica van gemengde gassen, is misleidend.

[1] R. Enderlein, G.M. Sipahi, L.M.R. Scolfaro en J.R. Leite, Phys. Rev. Lett. **79**, 3712 (1997).

[2] P.A. Bobbert, M. Kemerink en P.M. Koenraad, Phys. Rev. Lett. **80**, 3159 (1998).

VII.

De geluidskwaliteit van een klarinetrietje wordt niet bepaald door de grootte en de getalsmatige dichtheid van de vaatbundels in de rietplant, die gebruikt wordt voor de fabricage van het klarinetrietje, maar door de specifieke samenstelling van de vaatbundels.

[1] P. Kolesik, A. Mills en M. Sedgley, Anatomical Characteristics Affecting the Musical Performance of Clarinet Reeds made from *Arundo donax* L. (Gramineae), *Annals of Botany* **81**, 151 (1998).

VIII.

Gezien het feit dat de kinetische energie van een bewegend lichaam evenredig is met het kwadraat van de snelheid verdient het aanbeveling de boetes voor snelheidsovertredingen daarmee gelijke tred te laten houden.

IX.

Het stemmen van zwevende kiezers bij verkiezingen lijkt op het resultaat van een kwantummechanische meting. Het is wellicht beter de kiezer de mogelijkheid te geven om op een superpositie van partijen te stemmen.

X.

De invoering van een tweede scheidsrechter bij een voetbalwedstrijd, die zich wellicht buiten het voetbalveld zou bevinden en die de mogelijkheid zou krijgen om gebruik te maken van moderne waarnemingstechnieken, zou een gunstiger uitslag voor de minder favoriete ploegen tot gevolg hebben.

[1] WK '98 voetbalwedstrijd Italië — Chili (2 — 2), 11 juni 1998.

XI.

De recente uitspraak van computergigant Hewlett Packard, dat het tijdperk van kwantumcomputers aanbreekt omdat in het jaar 2010 de limiet van schaalverkleining in de conventionele silicium computertechnologie zal worden behaald, is nogal voorbarig: als het al mogelijk is deze praktisch te realiseren, dan zal het minstens nog meerdere decennia duren voordat de eerste serieuze kwantumcomputer wordt gebouwd.

[1] Persbericht Hewlett Packard.

XII.

De invoering van de euro en het concept van “klantvriendelijke” (psychologische) prijzen gaan slecht samen.

XIII.

De benaming van de laatste Mondriaan geeft goed weer hoe de vorige eigenaar van dit doek zich momenteel wellicht zal voelen.